PHILOSOPHICAL TRANSACTIONS OF THE ROYAL SOCIETY A MATHEMATICAL, PHYSICAL & ENGINEERING SCIENCES

The Propagation of Plane Irrotational Waves through an Elastoplastic Medium

L. W. Morland

Phil. Trans. R. Soc. Lond. A 1959 **251**, 341-383
doi: 10.1098/rsta.1959.0006

THE PROPAGATION OF PLANE IRROTATIONAL WAVES THROUGH AN ELASTOPLASTIC MEDIUM

By L. W. MORLAND*

Department of Mathematics, Manchester University

(*Communicated by M. J. Lighthill, F.R.S.—Received* 8 *August* 1958)

CONTENTS

This paper is an attempt at a systematic investigation of wave propagation in a metal, treating interactions between elastic and plastic waves, and the formation and propagation of shock waves, in the general case of motions with unidirectional strain arising from an initial smooth loading-unloading pulse. A stress-strain relation with linear elastic paths and concave-upward plastic paths (where compression is measured as positive) is derived and used so that the elastic wave velocity is uniform, and the plastic wave velocity an increasing function of stress. The analysis is in terms of engineering stress and strain with a Lagrangian co-ordinate system.

Analytic solutions to the interactions between different types of continuous waves are developed incorporating an expression for the motion of the elastic-plastic boundary. An analysis of the breakdown of a smooth plastic compression wave into a shock wave is presented, and the propagation conditions derived. It is shown that the heat dissipated is proportional to the cube of the strain jump, its low value for moderate shock strength suggests that the shock does not appreciably affect the stress-strain relation, an assumption from which a solution for the unloading of a plastic compression front by an overtaking elastic wave, while shock formation is taking place, is derived. A numerical illustration of this solution for a particular pulse in aluminium is given.

INTRODUCTION

To bring out the main physical features involved in the formation and propagation of shock waves in solids, and in interactions of elastic and plastic waves in general, and particularly because the parallel investigation in gas dynamics, initiated by Riemann, proved of such

* Now at Applied Mathematics Division, Brown University, Providence 12, Rhode Island, U.S.A.

fundamental suggestive value in that science, this paper attempts a systematic treatment of the propagation of a one-dimensional pulse of general shape in a metal. This wave system with pure longitudinal strain corresponds to the motion initiated in a semi-infinite block by a normal force applied uniformly over the free surface. It is considered an adequate approximation by experimentalists for pulses propagated across thin plates by impulsive loading, when the travel time is too small for appreciable lateral displacement. Such work (Pack, Evans & James 1948; Mallory 1955; Walsh & Christian 1955) has shown the formation of plane shock waves for various metals. This paper treats the interactions between continuous elastic and plastic waves, analyses the continuous breakdown of a plastic compression wave into a shock wave, and treats the elastic unloading of such a wave whilst the shock formation is taking place. These are events in the wave system initiated by a smooth loading-unloading pulse.

An important aspect is the derivation of a longitudinal stress-strain relation, which, for the continuous waves, should represent an adiabatic equation of state. Excluding the metals exhibiting upper and lower yield points, such as mild steel, the plastic yielding and reverse yielding stress-strain relations are shown to depend on a hydrostatic compresssion term plus a comparatively smaller simple compression (or tension) term, while elastic changes satisfy the generalized Hooke's law. These results are obtained by modifying a method of Wood (1952) to allow for the variation of the elastic parameters with increasing pressure. Bridgman's (1949*a*, *b*) quasi-static isothermal experiments have determined the bulk modulus for many metals up to very high pressure, and show it to be an increasing function of pressure, while the results for the shear modulus are not so accurate but show that the variation is comparatively smaller. In consequence, the plastic sections of the stress-strain curve (measured positive in compression) are concave upwards, while, since the variation of the moduli over the small elastic ranges is negligible, the elastic sections are adequately linear. Since there are no extensive data on the results of temperature increase and rate of strain increase on the moduli, a relationship neglecting these is adopted. It is expected that at the higher rates of strain the upward curvature of the stress-strain path will be increased, but the approximation does not alter the form of the wave interaction solutions nor the analysis of continuous wave breakdown, but only affects various calculated shock quantities. The wave velocity (Lagrangian) is proportional to the square root of the approximate stress-strain gradient, and so elastic wave velocity is uniform and plastic wave velocity an increasing function of stress.

Donnell (1930) mentioned the continuous change in shape of a plastic wave due to the non-linear stress-strain relation, but the first complete treatment of plastic wave propagation in a bar was given by Karman, Bohnenblust & Hyers (1942), the simple compression-tension plastic stress-strain curve being concave downwards. White & Griffis (1948) point out the breakdown of a continuous wave into a shock for a concave-upward stress-strain curve. The interactions and resulting permanent-strain distribution caused by longitudinal impact of a long uniform bar are treated by White & Griffis (1947) using characteristics, and similarly for a finite bar, considering reflexions, by Lee (1952), Lee & Tupper (1954), and Broberg (1955). Koehler & Seitz (1944) treat the propagation through a plate of a pulse with sharp loading front and smooth release, but ignore the reverse yielding which occurs after limited elastic unloading in a longitudinal strain system. Lee (1952) emphasizes the high

degree of numerical accuracy required in determining the elastic-plastic boundary. These solutions assume constant plastic wave velocity.

In this paper, the propagation of smooth pulses is treated, allowing for non-uniform plastic wave velocity, and a method of obtaining the continuous solution to an interaction between elastic and plastic waves is developed; that is, the distributions of stress, strain, and particle velocity over the region throughout the interaction are obtained analytically, and in particular, an expression for the elastic-plastic boundary (or interaction path) is derived. This latter result is particularly useful. The continuous distribution of permanent strain left over the interaction region is derived in the above solution. The overtaking of a plastic loading wave by an elastic unloading wave is dealt with in detail, and another similar case summarized to show the ready extension of the method. Shock propagation is next considered, and the breakdown of a continuous plastic loading wave into a series of elementary shocks, and finally into a single stable shock, is described; the analysis deriving the shock front path, or paths, during the breakdown being based on an observation by Lighthill (1956). On the assumption that the shock does not appreciably alter the original adiabatic stress-strain relation, a solution for the elastic unloading of the plastic front during the breakdown into shock is derived. It has the same analytic form as the solution not involving breakdown, but differs in the derivation of the interaction path at each stage which depends on the shock-front analysis. This combined interaction-breakdown solution is illustrated numerically for a particular pulse.

Notation

Using rectangular Cartesian axes, the axis Ox is chosen in the direction of flow.

x is a Lagrangian co-ordinate, defining the initial position of a particle; u is the displacement of the particle.

t denotes time.

$t = 0$ is taken as the starting time of the first unloading interaction;

$t = t_s$ is the time at commencement of shock formation, and

$t = t_c$ is the time at completion of shock formation across the plastic front assuming no interference from the elastic unloading wave;

$t = t_f$ is the time at the end of the first unloading interaction (with or without shock formation).

ϵ_j is a principal engineering strain, defined as the change in length per unit initial length of element in the j-direction.

σ_j is a principal engineering stress, defined as the force in the j-direction per unit initial area of cross-section whose normal is in the j-direction.

For convenience, stress and strain are measured positive in compression, contrary to the usual convention. The material is assumed to be isotropic, and so the principal axes of stress and strain coincide. Referring to principal stress in the x-direction: σ_Y denotes the initial yield stress, σ_m the maximum applied stress, $\sigma_{Y'}$ the reverse yield stress, and σ_r the reduced maximum stress of the plastic front on completion of the first unloading interaction.

The same suffixes are used to denote the corresponding strain levels.

E is Young's modulus.

ν is Poisson's ratio.

PHILOSOPHICAL TRANSACTIONS OF THE ROYAL SOCIETY A MATHEMATICAL, PHYSICAL & ENGINEERING SCIENCES

K is the bulk modulus.
μ is the shear modulus.
ρ denotes density.
V denotes specific volume.
v denotes particle velocity.
U is internal energy per unit mass.
c_0 and c_1 denote Lagrangian elastic and plastic wave velocity, respectively.

I. BASIC EQUATIONS

1. Equations of motion

The flow is unidirectional, along Ox; from symmetry, the dependent variables can be expressed as functions of the Langrangian co-ordinates (x, t) alone. The compressive engineering strain is defined by

$$\epsilon_x = -\partial u/\partial x, \tag{1·1}$$

where u is the particle displacement. Note that this definition requires differentiation with respect to the original co-ordinate of a particle.

Conservation of mass requires that

$$\rho(1-\epsilon_x) = \rho_i, \tag{1·2}$$

where ρ is the current density, and ρ_i the initial density.

Conservation of momentum gives

$$\frac{\partial^2 u}{\partial t^2} = -\frac{1}{\rho_i}\frac{\partial \sigma_x}{\partial x}, \tag{1·3}$$

where σ_x is the principal engineering stress (compressive) in the x-direction. In general, to satisfy the stress-strain laws, there must exist a non-zero isotropic lateral stress $\sigma_y(x, t)$.

Assuming that there exists a longitudinal stress-strain relation, $\sigma_x = \sigma_x(\epsilon_x)$, which is verified in §2, (1·3) can be written

$$\frac{\partial^2 u}{\partial t^2} + \frac{1}{\rho_i}\frac{\mathrm{d}\sigma_x}{\mathrm{d}\epsilon_x}\frac{\partial \epsilon_x}{\partial x} = 0. \tag{1·4}$$

Using (1·1), this becomes

$$\frac{\partial^2 u}{\partial t^2} - c^2(\epsilon_x)\frac{\partial^2 u}{\partial x^2} = 0, \tag{1·5}$$

where

$$c^2(\epsilon_x) = \frac{1}{\rho_i}\frac{\mathrm{d}\sigma_x}{\mathrm{d}\epsilon_x}. \tag{1·6}$$

For constant $c(\epsilon_x)$, (1·5) is the wave equation, and will be so described for the general case of non-uniform $c(\epsilon_x)$. $c(\epsilon_x)$ is the wave velocity in the Lagrangian system. This equation has positive and negative characteristics given by

$$\mathrm{d}x/\mathrm{d}t = \pm c(\epsilon_x). \tag{1·7}$$

It is easily verified that along $\mathrm{d}x/\mathrm{d}t = +c(\epsilon_x)$, a positive characteristic,

$$\frac{\partial u}{\partial t} - \int^u c(\epsilon_x)\, d\left(\frac{\partial u}{\partial x}\right) = \text{constant}, \tag{1·8}$$

and similarly, along a negative characteristic, $\mathrm{d}x/\mathrm{d}t = -c(\epsilon_x)$,

$$\frac{\partial u}{\partial t} + \int^{u} c(\epsilon_x)\, d\left(\frac{\partial u}{\partial x}\right) = \text{constant}. \tag{1·9}$$

That is, along $\mathrm{d}x/\mathrm{d}t = +c(\epsilon_x)$ and $\mathrm{d}x/\mathrm{d}t = -c(\epsilon_x)$,

$$v + \int^{\epsilon_x} c(\epsilon_x)\, \mathrm{d}\epsilon_x \quad \text{and} \quad v - \int^{\epsilon_x} c(\epsilon_x)\, \mathrm{d}\epsilon_x$$

are respectively constant, where $v = \partial u/\partial t$ is the velocity of a particle. Define the invariant on a positive characteristic as

$$R_1 = v + \int^{\epsilon_x} c(\epsilon_x)\, \mathrm{d}\epsilon_x, \tag{1·10}$$

and the invariant on a negative characteristic as

$$R_2 = v - \int^{\epsilon_x} c(\epsilon_x)\, \mathrm{d}\epsilon_x. \tag{1·11}$$

In general, R_1 and R_2, are different on different characteristics.

If the pulse is propagating into a uniform region, then each negative characteristic passes through a section of the $x-t$ plane, corresponding to this uniform region, in which the flow variables, v and ϵ_x are constant. Therefore, the invariant R_2 is identical for all negative characteristics, and can be replaced by an absolute constant R. Hence, along each positive characteristic, which is intersected at every point by some negative characteristic,

$$\left.\begin{aligned} v + \int^{\epsilon_x} c(\epsilon_x)\, \mathrm{d}\epsilon_x &= R_1, \\ v - \int^{\epsilon_x} c(\epsilon_x)\, \mathrm{d}\epsilon_x &= R. \end{aligned}\right\} \tag{1·12}$$

Addition and subtraction show that v and $\int^{\epsilon_x} c(\epsilon_x)\, \mathrm{d}\epsilon_x$ are separately constant on each positive characteristic, and by the appropriate choice of the lower limit of the integral

$$v = \int^{\epsilon_x} c(\epsilon_x)\, \mathrm{d}\epsilon_x. \tag{1·13}$$

Furthermore, since $\int^{\epsilon_x} c(\epsilon_x)\, \mathrm{d}\epsilon_x$ is a function of ϵ_x only, and is an increasing function since $c(\epsilon_x) > 0$, ϵ_x must also be constant on each positive characteristic. It follows that the dependent variables, $c(\epsilon_x)$, $\sigma_x(\epsilon_x)$, also remain constant, and so each positive characteristic has a constant slope $\mathrm{d}x/\mathrm{d}t = c(\epsilon_x)$. This simple wave solution applies to a pulse propagating into a uniform region throughout which there is a common stress-strain relation $\sigma_x(\epsilon_x)$. In particular, if the stress-strain relation is linear, so that the wave velocity $c(\epsilon_x)$ is uniform, then each positive characteristic has the same constant slope $\mathrm{d}x/\mathrm{d}t = c$. Since σ_x is constant on each positive characteristic, the stress distribution $\sigma_x(x, t)$ will then have the form $f(x-ct)$.

An alternative case which arises in the interaction problems is that for a stress-strain relation $\sigma_x(\epsilon_x, x)$, that is, when successive particles follow different stress-strain paths. We differentiate (1·3) partially with respect to x to give

$$\frac{\partial^2 \epsilon_x}{\partial t^2} = \frac{1}{\rho_i} \frac{\partial^2 \sigma_x}{\partial x^2}, \tag{1·14}$$

and the stress-strain relation twice with respect to t to give

$$\frac{\partial^2\sigma_x}{\partial t^2} = \left(\frac{\partial\sigma_x}{\partial\epsilon_x}\right)_x \frac{\partial^2\epsilon_x}{\partial t^2} + \frac{\partial}{\partial t}\left(\frac{\partial\sigma_x}{\partial\epsilon_x}\right)_x \frac{\partial\epsilon_x}{\partial t}. \tag{1·15}$$

In the case when the stress-strain relation for all particles has a common linear gradient, that is, $\partial\sigma_x/\partial\epsilon_x$ is constant, then (1·14) and (1·15) give

$$\frac{\partial^2\sigma_x}{\partial t^2} = c^2\frac{\partial^2\sigma_x}{\partial x^2}, \tag{1·16}$$

where $c^2 = (1/\rho_i)\,\mathrm{d}\sigma_x/\mathrm{d}\epsilon_x$ is constant. The solution is therefore given in terms of a stress distribution which has the form

$$\sigma_x(x,t) = g(x-ct)+h(x+ct), \tag{1·17}$$

which represents stress waves propagating in both directions.

The above two types of solution to the wave equation are sufficient for the continuous wave propagation system considered. Shock propagation conditions are treated in part III. Changes produced by the rapid continuous pulses are assumed adiabatic, and so the required relation $\sigma_x(\epsilon_x)$ is an adiabatic equation of state. Its derivation is treated in the next section.

One further useful result is the expression for particle velocity obtained by integrating (1·3), namely

$$v-v_0 = \frac{1}{\rho_i}\int_{t_0}^{t}\left(\frac{\partial\sigma_x}{\partial x}\right)_x \mathrm{d}t. \tag{1·18}$$

2. The longitudinal stress-strain relation

As shown in § 1, the solution to the equation of motion depends on the appropriate stress-strain relation, $\sigma_x(\epsilon_x)$. It is assumed that the rapid changes produced by the waves are adiabatic, and therefore an adiabatic equation of state is required. The stress-strain path in question is that followed by the material when σ_x is increased compressively from zero to some plastic level, and then decreased back to zero. Now stress-strain relations have been obtained accurately only for simple loading tests performed quasi-statically and isothermally. In this section then, a quasi-static isothermal longitudinal stress-strain path is derived in terms of data from hydrostatic compression and simple compression tests. This relation is then adopted as representing the required equation of state, after a brief discussion of rate-of-strain and temperature effects.

Wood (1952) has given a method for constructing a stress-strain path for a longitudinal strain system, which shows that the plastic loading relation depends mainly on an equivalent hydrostatic compression term. It is found, for metals in general, that the bulk modulus, K, increases with pressure, and, consequently, the related elastic parameters, E and ν, Young's modulus and Poisson's ratio, respectively, will vary also. In the following analysis, Wood's construction is modified by the use of differential relations to allow for the dependence of E and ν on density. Natural stress and strain are used without introducing new notation, although it is made clear when the transformation to engineering stress and strain is made. This is because elastic-plastic theory is usually treated in terms of natural stress and strain, which are defined with respect to the current configuration of an element.

Excluding mild steel and the hexagonal metals, the typical stress-strain path for a simple compression-tension test is depicted in figure 1. Neglecting a slight hysteresis loop for unloading-reloading, $SV-VS$, elastic paths such as SV and OP are reversible. Unloading beyond V produces reverse yielding VW; the reverse yield stress is either equal in magnitude to that at S, the previous yield point, or less if the material exhibits a Bauschinger effect. Reloading from any state on VW is elastic until the previous yield path, PS, is reached. A full account is given by Hill (1950).

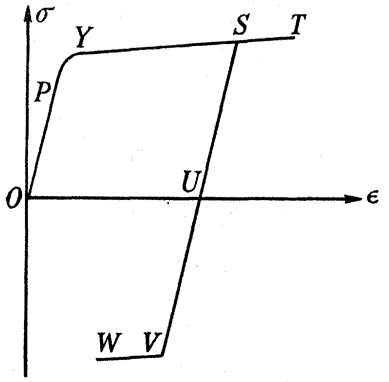

FIGURE 1. Simple compression-tension stress-strain path.

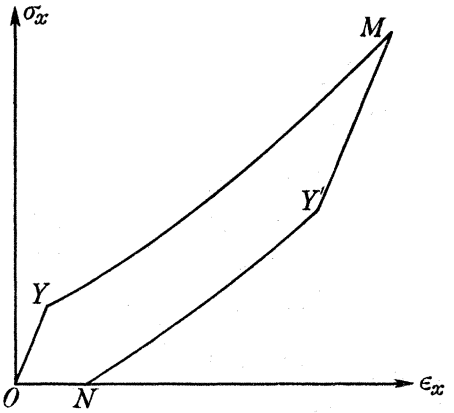

FIGURE 2. Longitudinal stress-strain path.

Incremental elastic changes are governed by the generalized Hooke's law:

$$E\,\mathrm{d}\epsilon_x^e = \mathrm{d}\sigma_x - 2\nu\,\mathrm{d}\sigma_y, \tag{2·1}$$

$$E\,\mathrm{d}\epsilon_y^e = (1-\nu)\,\mathrm{d}\sigma_y - \nu\,\mathrm{d}\sigma_x. \tag{2·2}$$

In the longitudinal strain system of this paper, all directions y orthogonal to Ox are identical principal axes, and the normal strain in any of these directions is zero. Referring to figure 2, the initial increase of σ_x up to the yield stress σ_Y, along OY, is elastic and so given by

$$\mathrm{d}\sigma_y = \frac{\nu}{1-\nu}\,\mathrm{d}\sigma_x, \tag{2·3}$$

$$\mathrm{d}\sigma_x = \frac{E(1-\nu)}{(1-2\nu)\,(1+\nu)}\,\mathrm{d}\epsilon_x, \tag{2·4}$$

since $\epsilon_y \equiv 0$. On further loading, YM, plastic yielding occurs, and both Von Mises's and Tresca's yield criterions reduce to

$$\sigma_x - \sigma_y = f(W_p), \tag{2·5}$$

where $f(W_p)$ is a function of the plastic (irreversible) work done. The total strain increment, $d\epsilon$, may be split into two components; $d\epsilon^e$, elastic and reversible, and $d\epsilon^p$, plastic and permanent; thus

$$d\epsilon_x = d\epsilon_x^e + d\epsilon_x^p, \tag{2·6}$$

$$d\epsilon_y = d\epsilon_y^e + d\epsilon_y^p. \tag{2·7}$$

The elastic strain increments satisfy (2·1) and (2·2); and the plastic strain increments satisfy the condition that no density change is produced, expressed by

$$0 = d\epsilon_{ii}^p = d\epsilon_x^p + 2\,d\epsilon_y^p. \tag{2·8}$$

The plastic work done per unit volume in producing a plastic strain increment $d\epsilon_x^p$ is

$$dW_p = \sigma_x\,d\epsilon_x^p + 2\sigma_y\,d\epsilon_y^p, \tag{2·9}$$

which becomes, on substituting for $d\epsilon_y^p$ from (2·8)

$$dW_p = (\sigma_x - \sigma_y)\,d\epsilon_x^p = f(W_p)\,d\epsilon_x^p. \tag{2·10}$$

In simple compression, the yield criterion reduces to

$$\sigma_x = f(W_p), \tag{2·11}$$

and the plastic work done per unit volume in producing the same plastic strain increment $d\epsilon_x^p$ is

$$dW_p = \sigma_x\,d\epsilon_x^p = f(W_p)\,d\epsilon_x^p. \tag{2·12}$$

Since both plastic loading sections, PT in figure 1 and YM in figure 2, start with $\epsilon_x^p = 0$, the plastic work done in producing a given plastic strain ϵ_x^p is the same for both systems. Thus, if the plastic loading curve in simple compression is defined by $\sigma = \sigma_s(\epsilon_x^p)$, then from (2·11) the yield criterion (2·5) may be expressed as

$$\sigma_x - \sigma_y = \sigma_s(\epsilon_x^p). \tag{2·13}$$

It follows that incremental changes during plastic yielding satisfy

$$d\sigma_x - d\sigma_y = d\sigma_s. \tag{2·14}$$

Putting $\epsilon_y \equiv 0$ in (2·7) and combining with (2·8),

$$d\epsilon_y^e = \tfrac{1}{2}\,d\epsilon_x^p. \tag{2·15}$$

Using this relation in (2·2),

$$d\sigma_y = \frac{\nu}{1-\nu}\,d\sigma_x + \frac{E}{2(1-\nu)}\,d\epsilon_x^p. \tag{2·16}$$

Eliminating $d\sigma_y$ between (2·14) and (2·16),

$$d\sigma_x = \frac{1-\nu}{1-2\nu}\,d\sigma_s + \frac{E}{2(1-2\nu)}\,d\epsilon_x^p. \tag{2·17}$$

Eliminating $d\epsilon_x^e$ between (2·1) and (2·6), and substituting for $d\sigma_y$ by (2·14),

$$d\epsilon_x^p = d\epsilon_x - \{(1-2\nu)\,d\sigma_x + 2\nu\,d\sigma_s\}/E. \tag{2·18}$$

The longitudinal stress-strain relation for the initial plastic loading is given in differential form by eliminating $\mathrm{d}\epsilon_x^p$ between (2·17) and (2·18):

$$\mathrm{d}\sigma_x = \frac{E}{3(1-2\nu)}\,\mathrm{d}\epsilon_x + \tfrac{2}{3}\,\mathrm{d}\sigma_s. \tag{2·19}$$

Now, except perhaps for a short range PY (figure 1), $E\,\mathrm{d}\epsilon_x$ is very large compared with $\mathrm{d}\sigma_s$; that is, the effect of work hardening is comparatively small. We make the approximation $\mathrm{d}\sigma_s \equiv 0$, and so $\sigma_s = Y =$ constant, where Y is the yield stress in simple compression; this is the exact representation of a perfectly plastic material. The plastic yielding equation becomes

$$\frac{\mathrm{d}\sigma_x}{\mathrm{d}\epsilon_x} = \frac{E}{3(1-2\nu)}. \tag{2·20}$$

The factor $E/3(1-2\nu)$ is now required as a function of ϵ_x. Consider an incremental hydrostatic compression $\mathrm{d}p$ producing an increase $\mathrm{d}\epsilon_h$ in each of the three identical principal compressive strains ϵ_h; the volume decrease is given by

$$-\mathrm{d}V/V = 3\,\mathrm{d}\epsilon_h. \tag{2·21}$$

The change is purely elastic, and applying (2·1) gives

$$3(1-2\nu)\,\mathrm{d}p = -E\,\mathrm{d}V/V. \tag{2·22}$$

Therefore, by (2·20) and (2·21), the plastic yielding equation is

$$\frac{\mathrm{d}\sigma_x}{\mathrm{d}\epsilon_x} = -V\frac{\mathrm{d}p}{\mathrm{d}V} = K, \tag{2·23}$$

where K is the bulk modulus. A hydrostatic compression formula incorporating two parameters, α and β, deduced from quantum mechanics, has been fitted over large pressure ranges for many metals by Bridgman (1949*a*); the data were obtained isothermally. The formula is

$$p = \alpha\left(\frac{V_i}{V}\right)^{\frac{2}{3}}\left\{\exp\left[\beta\frac{V_i^{\frac{1}{3}}-V}{V_i^{\frac{1}{3}}}\right]-1\right\}, \tag{2·24}$$

where V is the specific volume with V_i the unstrained value. This will be applied when (2·23) has been modified to engineering stress and strain.

Unloading from a state M (figure 2) is elastic until the reverse yield point Y' is reached; the governing equation is therefore (2·4). Introducing the elastic parameters K, the bulk modulus, and μ, the shear modulus, provides alternative expressions for E and ν:

$$K = \frac{E}{3(1-2\nu)}, \quad \mu = \frac{E}{2(1+\nu)}, \tag{2·25}$$

$$E = \frac{9\mu K}{\mu+3K}, \qquad \nu = \frac{3K-2\mu}{2(\mu+3K)}. \tag{2·26}$$

The elastic relation, (2·4), becomes

$$\mathrm{d}\sigma_x/\mathrm{d}\epsilon_x = K + \tfrac{4}{3}\mu. \tag{2·27}$$

Reverse yielding for unloading beyond Y' is governed by (2·23), since the analysis still applies; the only difference appears in the new origin of integration.

At this stage we revert to engineering stress and strain, σ_x and ϵ_x, and denote natural stress and strain by a suffix n, Then, for longitudinal strain, $\sigma_x \equiv \sigma_{xn}$ and $\mathrm{d}\epsilon_x = (1-\epsilon_x)\,\mathrm{d}\epsilon_{xn}$. The plastic yielding equation (2·23) becomes

$$\frac{\mathrm{d}\sigma_x}{\mathrm{d}\epsilon_x} = \frac{K}{1-\epsilon_x}, \tag{2·28}$$

and the elastic relation (2·27) becomes

$$\frac{\mathrm{d}\sigma_x}{\mathrm{d}\epsilon_x} = \frac{K+\frac{4}{3}\mu}{1-\epsilon_x}. \tag{2·29}$$

Using the continuity equation $V = V_i(1-\epsilon_x)$, (2·30)

the plastic equation (2·28) becomes further

$$\frac{\mathrm{d}\sigma_x}{\mathrm{d}\epsilon_x} = \frac{K}{1-\epsilon_x} = \frac{\mathrm{d}p}{\mathrm{d}\epsilon_x}, \tag{2·31}$$

and (2·24) gives $p = \alpha(1-\epsilon_x)^{-\frac{2}{3}}\{\exp[\beta\{1-(1-\epsilon_x)^{\frac{1}{3}}\}]-1\}$. (2·32)

The longitudinal stress-strain relation can now be expressed explicitly. Denote the initial and reverse yield points by the superscripts (Y) and (Y'), respectively, and the maximum stress point before unloading by (M). From (2·31) the plastic loading relation is

$$\sigma_x - \sigma_x^{(Y)} = p(\epsilon_x) - p[\epsilon_x^{(Y)}]. \tag{2·33}$$

Comparing (2·29) and (2·31), and assuming μ to be constant—this is discussed towards the end of this section—the appropriate elastic relations are

$$0 \leqslant \sigma_x \leqslant \sigma_x^{(Y)}: \quad \sigma_x = p(\epsilon_x) - \tfrac{4}{3}\mu \ln(1-\epsilon_x), \tag{2·34}$$

$$\sigma_x^{(Y')} \leqslant \sigma_x \leqslant \sigma_x^{(M)}: \quad \sigma_x^{(M)} - \sigma_x = p[\epsilon_x^{(M)}] - p(\epsilon_x) - \tfrac{4}{3}\mu \ln\left[\frac{1-\epsilon_x^{(M)}}{1-\epsilon_x^{(Y')}}\right]. \tag{2·35}$$

It remains to determine the yield values $\epsilon_x^{(Y)}$, $\sigma_x^{(Y)}$, and $\epsilon_x^{(Y')}$, $\sigma_x^{(Y')}$. Using (2·3) and (2·4), the elastic paths satisfy

$$\mathrm{d}(\sigma_{xn} - \sigma_{yn}) = 2\mu\,\mathrm{d}\epsilon_{xn}. \tag{2·36}$$

Now the initial yield point is given by

$$\sigma_{xn} - \sigma_{yn} = Y, \tag{2·37}$$

and the reverse yield point, assuming no Bauschinger effect, by

$$[\sigma_{xn} - \sigma_{yn}]_{Y'}^{M} = 2Y. \tag{2·38}$$

Hence, translating into engineering stress and strain,

$$\left.\begin{aligned} \frac{Y}{2\mu} &= \int_0^{\epsilon_x^{(Y)}} \frac{\mathrm{d}\epsilon_x}{1-\epsilon_x}, \\ \frac{Y}{\mu} &= \int_{\epsilon_x^{(Y')}}^{\epsilon_x^{(M)}} \frac{\mathrm{d}\epsilon_x}{1-\epsilon_x}, \end{aligned}\right\} \tag{2·39}$$

and therefore, $\epsilon_x^{(Y)} = 1 - \exp(-Y/2\mu)$, (2·40)

$$1-\epsilon_x^{(Y')} = [1-\epsilon_x^{(M)}]\exp(Y/\mu). \tag{2·41}$$

The reverse yield point depends on the maximum stress point before unloading. The corresponding yield stresses, $\sigma_x^{(Y)}$ and $\sigma_x^{(Y')}$ are given by substitution in (2·34) and (2·35).

Bridgman (1949*b*) has found for metals in general that the shear modulus also increases with hydrostatic pressure, but the effect is less than for the bulk modulus; furthermore, it is difficult to obtain accurate results. Hence, we make the assumption $\mu =$ constant for isothermal compression. Comparing (2·29) and (2·31), it is clear that the elastic unloading path is more steep than the adjoining plastic loading section, and so the elastic unloading wave velocity is greater than the plastic loading wave velocity for each stress point. At some pressure, the plastic loading curves may become steeper than the initial loading line, but the above result is still valid.

Now there is a varying high rate of strain across the wave fronts, and this may affect the stress-strain relationship. Dynamic loading experiments have indicated a rise in the simple compression stress-strain curve; Johnson, Wood & Clark (1953) report for 2*S*-aluminium a rise above the static stress value increasing from zero at the elastic limit to about 20 % at a strain of 0·04, using impact velocities in the range 20 to 120 ft./s. There is difficulty in unravelling stress-strain properties from the wave propagation effects in dynamic experiments, and consequently difficulty in deriving accurate conclusions. Since the major contribution to the longitudinal plastic stress-strain relation is provided by the hydrostatic compression term, it is possible that this rise will not appreciably affect the curvature of the stress-strain path, nor the dependent plastic wave velocity.

Further, there will be a varying temperature distribution across the waves, which could also affect the elastic parameters. In general, at normal pressures, each of the elastic moduli shows a small decrease with temperature rise, which suggests a tendency for the upward curvature of the plastic loading path to decrease with temperature rise. For lack of any extensive data, the effect is neglected.

Finally, then, the upward curvature of the plastic yielding curve is determined from the known isothermal quasi-static bulk modulus variation, and that of the elastic paths is neglected.

II. THE CONTINUOUS WAVE SYSTEM INITIATED BY A SMOOTH LOADING-UNLOADING PULSE

3. Description of events

From now on, only the direction of flow is considered, and the suffix x is omitted. The form of pressure pulse applied at the free surface is shown in figure 3. The material is loaded compressively to a longitudinal stress σ_m, which is held constant for a short time, and then the material is unloaded until the longitudinal stress is again zero. From the stress-strain equations in §2, it can be shown that the lateral stress, on the other hand, is not completely removed; there is also a permanent longitudinal strain, represented by ϵ_N in figure 2.

It can now be seen how the disturbance propagates down the block; the references are to the stress-strain path in figure 2. Until the elastic limit σ_Y is reached, the pressure pulse travels as an elastic wave, and the amplitude is small. Owing to the slight upward curvature of the stress-strain path, the wave velocity will increase slightly with stress, and the elastic loading wave eventually becomes a weak shock. Shock propagation conditions are

developed in part III and it will be seen that such a weak shock is virtually equivalent to the original continuous wave except in its extent. Loading beyond the elastic limit is governed by the plastic yielding curve YM; the wave velocity $c_1(\epsilon)$ is an increasing function of strain, and in general is smaller than the velocity of the initial elastic wave. Thus, behind the preceding elastic wave there is an expanding uniform region at the elastic limit, into which the large-amplitude plastic loading wave propagates. The characteristics solution for a simple wave with non-uniform velocity is applicable to this plastic wave, since the material has a common stress-strain relation for initial plastic loading.

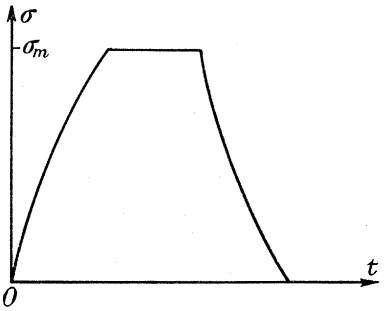

FIGURE 3. Applied pressure pulse at the free surface.

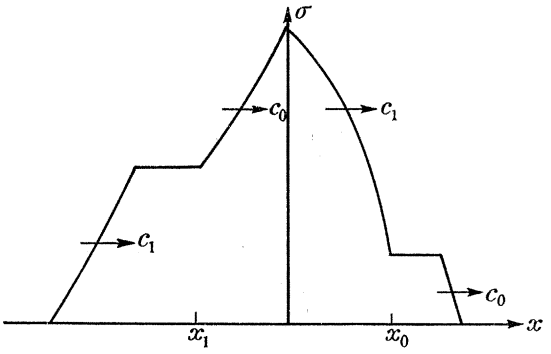

FIGURE 4. Stress-wave profile at start of first unloading interaction.

Behind the plastic loading front is a uniform region at the maximum stress σ_m, into which an elastic unloading wave, governed by the stress-strain path MY', propagates; this has greater velocity than the plastic wave, and therefore the region gradually contracts. In this case, the wave velocity increases with strain and causes the pulse to spread out, but since the variation is small over an elastic strain range, the unloading wave is taken to have a uniform velocity c_0; this will be greater than the initial elastic wave velocity as shown in § 2. Unloading below $\sigma_{Y'}$, until the longitudinal stress is removed, is governed by the reverse yielding path $Y'N$, and so propagates as a slower plastic wave; the pulse will tend to spread out. An expanding uniform region at stress $\sigma_{Y'}$ forms between the two unloading components. The situation is illustrated by a mapping of the respective wave characteristics of the applied pulse in an x-t plane shown in figure 5.

The preceding small amplitude elastic loading wave is only of interest in as much as it produces a uniform region at stress σ_Y into which the plastic loading wave propagates. The breakdown of the continuous plastic wave front and consequent shock propagation is

described in part III. Ignoring this for the present, the first event requiring special consideration will be the overtaking of the plastic loading wave by the faster elastic unloading wave. A solution to this interaction is obtained in three stages, §§ 4, 5 and 6; an incremental approach is used to develop the mechanism, treating each stress-wave profile as a series of small discontinuous steps with constant wave velocity; the resulting wave pattern is adapted, and a continuous solution is found; finally, an extension is made to a plastic wave with non-uniform velocity. Of the two main alternative cases, particular reference is made to

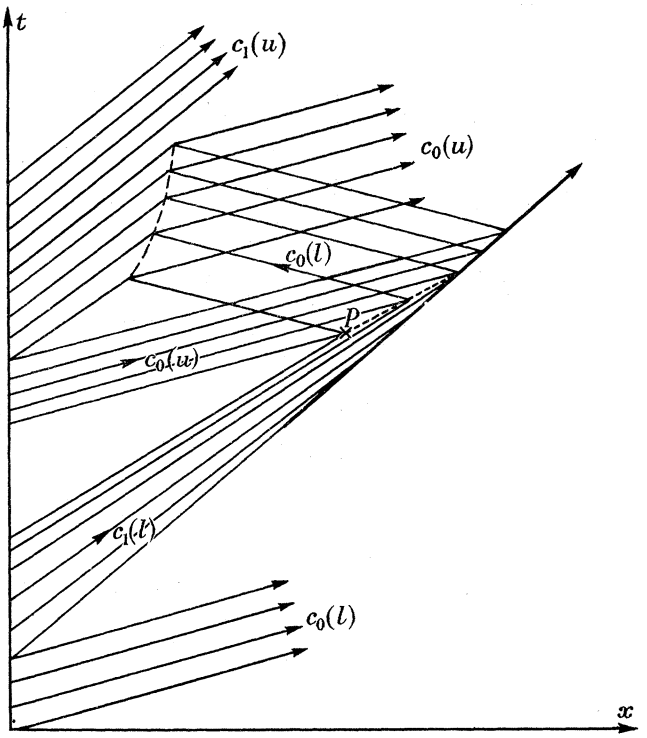

FIGURE 5. Characteristic diagram for wave system initiated by a smooth loading-unloading pulse, showing the shock path (—) and the elastic-plastic boundaries (– – –) for the first two interactions. (u) and (l) denote unloading and loading waves, respectively.

that applicable to a plastic wave of greater amplitude than the unloading wave. From (2·3), elastic changes satisfy

$$\mathrm{d}(\sigma_{xn}-\sigma_{yn}) = \frac{1-2\nu}{1-\nu}\,\mathrm{d}\sigma_{xn}. \tag{3·1}$$

Since in general, ν is roughly $\frac{1}{3}$, (2·38) gives

$$\sigma_m-\sigma_{Y'}\sim 4Y, \tag{3·2}$$

$$\sigma_{Y'}\sim 2Y. \tag{3·3}$$

Hence, $\sigma_m-\sigma_Y > \sigma_m-\sigma_{Y'}$ if $\sigma_m > 3\sigma_Y$ or $\sigma_m > 6Y$. This is the interesting case; it results in a reduced plastic loading wave continuing forward, and a reflected elastic loading wave. In the other case, the plastic loading wave is completely annulled, and an elastic unloading wave propagates forward; again, there is a reflected elastic loading wave. In both cases, the amplitude of the elastic loading wave is a small proportion of that of the initial elastic unloading wave, and the pulse length is a large multiple of the initial pulse length, so a slight variation of the wave velocity will not cause shock formation for a considerable time.

The reflected elastic loading wave meets the oncoming plastic unloading wave, and the solution to this second interaction is summarized in §7. There results an elastic unloading wave which propagates down the block, and will eventually overtake the reduced plastic loading front (if any); the treatment of this and further interactions is not given in detail, but the final outcome is described at the end of §7. For a moderate value of σ_m, the plastic unloading wave is not completely annulled, and the remaining wave follows the elastic unloading wave; the material behind is left with a permanent strain represented by ϵ_N in figure 2. Alternatively, when the plastic unloading wave is annulled, an elastic loading wave is propagated back to the free surface, where it is reflected as an elastic unloading wave; the material is again left with permanent strain ϵ_N.

The overtaking of the plastic loading wave while it is breaking down into a shock wave is treated in part III. The interaction is similar to that between the continuous elastic unloading and plastic loading waves; a reduced shock propagates forward and an elastic loading wave is reflected. The resulting wave amplitudes are the same. A numerical illustration to this general solution is given at the end of this paper.

Each of the stress-wave profiles before the interactions start is derived from the applied pressure pulse using the simple-wave solution. If the pressure pulse applied to the free surface, $x = 0$, shown in figure 3 is given by $\sigma = \sigma(t')$ or $t' = t'(\sigma)$, and $c(\sigma)$ denotes the wave velocity appropriate to an increment at stress σ, then since σ and $c(\sigma)$ are constant on tracks $\mathrm{d}x/\mathrm{d}t = c(\sigma)$, at a subsequent time t

$$x(\sigma) = c(\sigma)\,[t - t'(\sigma)], \tag{3·4}$$

where $x(\sigma)$ describes the stress profile at time t. This simple wave solution no longer holds once the interactions start.

For convenience, the x-t origin is chosen as the meeting point of the rear plastic loading wave characteristic and the leading elastic unloading wave characteristic, labelled P in figure 5; that is, the point at which the first interaction starts. Relation (3·4) can be adjusted to this system. The preceding elastic loading wave is replaced by a uniform stress region at the elastic limit, since it has no effect on the interaction; and the following plastic unloading wave is replaced by a uniform stress region at the reverse yield point for the purpose of solving the first interaction, since it plays no part. The initial stress distribution is described by

$$x \geqslant x_0: \quad \sigma = \sigma_Y, \tag{3·5}$$

$$\left.\begin{aligned} 0 \leqslant x \leqslant x_0: &\quad \sigma = F(x), \\ \sigma_Y \leqslant \sigma \leqslant \sigma_m: &\quad x = \mathscr{F}(\sigma), \end{aligned}\right\} \tag{3·6}$$

$$\left.\begin{aligned} -x_1 \leqslant x \leqslant 0: &\quad \sigma = G(x), \\ \sigma_{Y'} \leqslant \sigma \leqslant \sigma_m: &\quad x = \mathscr{G}(\sigma), \end{aligned}\right\} \tag{3·7}$$

$$x \leqslant -x_1: \quad \sigma = \sigma_{Y'}, \tag{3·8}$$

where x_0 is the length of the plastic loading-stress profile, and x_1 that of the elastic unloading-stress profile, at $t = 0$, and $\mathscr{F}$, $\mathscr{G}$ are inverse to F, G.

For the treatment of the second interaction between the elastic loading wave, reflected by the first interaction, and the oncoming plastic unloading wave, new initial conditions are required which depend on the above reflected wave profile. These are given in §7.

4. Interaction between a plastic loading wave and an overtaking elastic unloading wave—incremental approach

The solution to the interaction between the continuous plastic loading wave and the overtaking elastic unloading wave is developed in these next three sections. It applies to the case when the initial wave profiles are such that interaction is completed before the plastic front starts to break down into a shock wave; the more general case of combined unloading and shock formation is treated in part III. In this section an incremental approach is adopted to obtain a picture of the wave system produced during the interaction. The corresponding stress-wave forms are set up in § 5, and a continuous solution is derived; both elastic and plastic wave velocities are assumed constant in these sections. In § 6, the modification to the case of non-uniform plastic wave velocity is made, but elastic wave velocity is still taken as constant. The (x, t) origin is taken to be the meeting point of the two wave forms, represented by P in figure 5; the appropriate initial stress-wave profiles have been described in § 3, and are illustrated in figure 4.

The method of this section is to treat each stress-wave profile as a series of small discontinuous steps. Since both wave velocities are assumed to be uniform, these wavelets propagate with a constant velocity $\mathrm{d}x/\mathrm{d}t = c_0$ or c_1, where c_0 is elastic, and c_1 plastic, wave velocity. A stress increment $\delta\sigma$ propagating with velocity c produces a particle velocity change δv; this can be calculated from the relationship (1·18) by considering a pulse of length δx, and taking the limit as $\delta x \to 0$, with the result

$$\delta v = \pm \delta\sigma/\rho_i c. \tag{4·1}$$

The + sign is taken if the wave propagates in the positive direction, in which v is measured positive; and the − sign for the converse. The corresponding strain jump is, by definition of c

$$\delta\epsilon = \delta\sigma/\rho_i c^2. \tag{4·2}$$

The wavelet pattern resulting from an interaction between two wavelets must satisfy continuity of particle velocity and stress everywhere except on the actual wave fronts; in particular, continuity must be satisfied across the interaction line at later times. The resulting system must also be compatible with the stress-strain paths which respective particles will follow when subjected to stress changes by the passage of the wavelets. It is found in some cases, though, that, in order to satisfy the above conditions, strain discontinuities are created on the interaction line; their significance will be explained as the event arises. This technique is illustrated by White & Griffis (1949).

(*a*) *Meeting of elastic loading and unloading wavelets*

The interaction between elastic stress waves, assuming constant wave velocity, has a well-known solution which is given simply by addition of the wave functions as shown in (1·17). For completeness, the technique applied in (*b*) to the plastic wave interaction is also given in this case. The situation before and after the interaction is shown in figure 6; stress continuity is automatically satisfied. The initial unloading wavelet reduces the stress from σ_2 to σ_0, and the loading wavelet increases the stress from σ_2 to σ_1. α, β, represent particles immediately in front of, and behind, the interaction line which is initially at stress σ_2. σ_3, the stress produced

at the interaction line by the resulting wavelets, is determined in terms of the initial unloading and loading stress increments, Δ' and Δ, respectively, by applying continuity of particular velocity across $\alpha-\beta$ subsequent to the interactions. Let v_2 be the particle velocity in the uniform stress region between the approaching wavelets, then, after the interaction, using (4·1)

$$\left.\begin{aligned} v_\alpha &= v_2+\frac{\sigma_0-\sigma_2}{\rho_i c_0}-\frac{\sigma_3-\sigma_0}{\rho_i c_0},\\ v_\beta &= v_2-\frac{\sigma_1-\sigma_2}{\rho_i c_0}+\frac{\sigma_3-\sigma_1}{\rho_i c_0}. \end{aligned}\right\} \tag{4·3}$$

Putting $v_\alpha = v_\beta$ gives

$$\left.\begin{aligned} \sigma_3-\sigma_0 &= \sigma_1-\sigma_2 = \Delta,\\ \sigma_1-\sigma_3 &= \sigma_2-\sigma_0 = \Delta'. \end{aligned}\right\} \tag{4·4}$$

Thus the elastic increments pass through each other unchanged, but stepped to the appropriate stress level; they do not violate the yield criterion. Using (4·2) to find the strain at α and β after the interaction gives $\epsilon_\alpha = \epsilon_\beta$, and so the strain is continuous there. Similar results are obtained in the cases of two loading, or two unloading, elastic wavelets meeting, provided that the yield criterion is not violated.

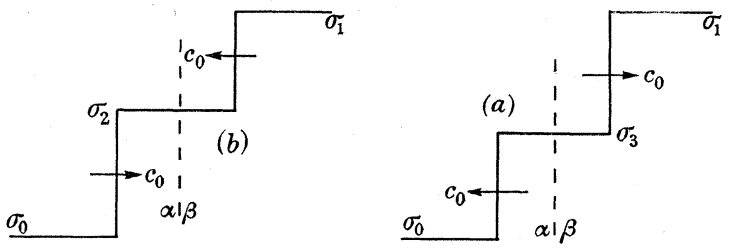

FIGURE 6. Situation before (*b*) and after (*a*) interaction between elastic loading and unloading increments.

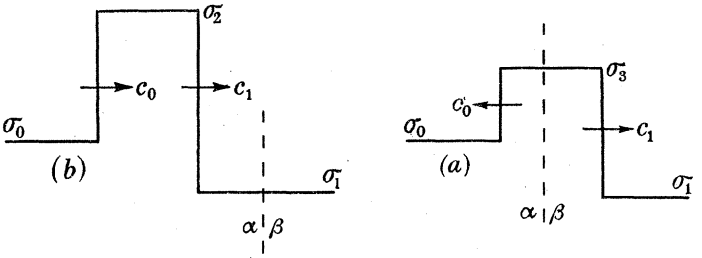

FIGURE 7. Situation before (*b*) and after (*a*) interaction between a plastic loading and an overtaking elastic unloading increment.

(*b*) *Overtaking of a plastic loading wavelet by an elastic unloading wavelet*

The situation is illustrated in figure 7; the interaction line α, β is ahead of both the initial wavelets. The plastic loading wavelet increases the stress from σ_1 to σ_2, and the elastic unloading wavelet reduces the stress from σ_2 to σ_0. The resulting wavelet pattern consists of a reduced plastic loading increment and a reflected elastic loading increment producing a stress σ_3 at the interaction line. The reflected wavelet has amplitude less than that of the initial elastic unloading wavelet, as will be shown, and is therefore elastic since the stress is throughout below the yield stress. The condition required on Δ' and Δ the initial unloading and loading increments, respectively, so that the forward wavelet is not unloading (when it

would be elastic) is found in the following analysis. Let the particle velocity in the uniform stress region ahead of the wavelets be v_1, then by (4·1)

$$\left.\begin{aligned} v_\alpha &= v_1+\frac{\sigma_2-\sigma_1}{\rho_i c_1}+\frac{\sigma_0-\sigma_2}{\rho_i c_0}-\frac{\sigma_3-\sigma_0}{\rho_i c_0}, \\ v_\beta &= v_1+\frac{\sigma_3-\sigma_1}{\rho_i c_1}. \end{aligned}\right\} \tag{4·5}$$

Putting $v_\alpha = v_\beta$ gives

$$\sigma_3-\sigma_0 = \frac{c_0-c_1}{c_0+c_1}\Delta', \tag{4·6}$$

which is positive independent of the ratio $\Delta':\Delta$; and

$$\sigma_3-\sigma_1 = \Delta-\frac{2c_1}{c_0+c_1}\Delta'. \tag{4·7}$$

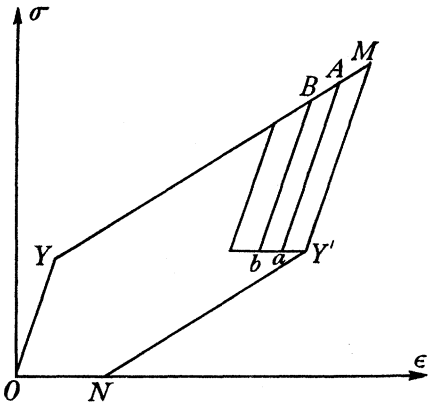

FIGURE 8. Elastic unloading paths, MY', Aa, ... after different amounts of plastic yielding.

The condition $\Delta' \leqslant (c_0+c_1)\,\Delta/2c_1$ is required since the adopted pattern has $\sigma_3-\sigma_1 \geqslant 0$. Let the strain in the forward uniform region be ϵ_1, then the strains at α and β are

$$\left.\begin{aligned} \epsilon_\alpha &= \epsilon_1+\frac{\Delta}{\rho_i c_1^2}-\frac{\Delta'}{\rho_i c_0^2}+\frac{c_0-c_1}{c_0+c_1}\frac{\Delta'}{\rho_i c_0^2}, \\ \epsilon_\beta &= \epsilon_1+\frac{\Delta}{\rho_i c_1^2}-\frac{2c_1}{c_0+c_1}\frac{\Delta'}{\rho_i c_1^2}, \end{aligned}\right\} \tag{4·8}$$

which give

$$\epsilon_\alpha-\epsilon_\beta = \frac{2c_1}{c_0+c_1}\frac{\Delta'}{\rho_i}\left(\frac{1}{c_1^2}-\frac{1}{c_0^2}\right) > 0. \tag{4·9}$$

Thus a negative strain discontinuity (in the direction of the initial wavelets) is introduced into the material at the interaction line, and since the stress is then continuous, this is a discontinuity in the plastic strain and so moves with the corresponding particle velocity. Another explanation of this discontinuity is afforded by inspecting the appropriate stress-strain paths in figure 8. Suppose the initial maximum stress, σ_2, is represented by M, and the reduced maximum plastic stress, σ_3, by A; then ϵ_α is calculated from elastic unloading-reloading along the path MY', and ϵ_β from the path Aa.

Let us consider the overall interaction by diving the elastic unloading wave into n equal stress increments Δ', and following the subsequent wavelet patterns. Since, by (4·7),

$\Delta-(\sigma_3-\sigma_1) = 2c_1\Delta'/(c_0+c_1)$, the first unloading wavelet is just sufficient to annul a plastic loading increment of size Δ given by

$$\Delta = \frac{2c_1}{c_0+c_1}\Delta'. \tag{4·10}$$

The reflected elastic loading wavelet has amplitude $\sigma_3-\sigma_0$ which is

$$\Delta'' = \frac{c_0-c_1}{c_0+c_1}\Delta'. \tag{4·11}$$

A strain discontinuity is created at the interaction line. The reflected elastic loading wavelet passed through the oncoming elastic unloading wavelets, leaving all stress increments unchanged; each wavelet is stepped in turn to the appropriate stress level. Before the second elastic unloading wavelet reaches the plastic form, it must pass through the strain discontinuity produced by the first interaction. Setting up a system of transmitted and reflected wavelets and a new strain discontinuity, it is easily shown that the unloading stress increment passes through unaltered, but with appropriate adjustment of strain level; that the reflected increment is zero (this is not true when the wave velocity varies with strain), and that the discontinuity has the same strain jump, and moves with the new particle velocity caused by the wavelet passing. This is equally true for an elastic loading increment. Hence, the second unloading wavelet will annul a second increment Δ of the plastic front, and a second elastic loading increment Δ'' is reflected. This pattern is repeated n times until the elastic unloading wave is annulled, provided that the plastic front is not annulled first; but if the latter event does occur, the remaining elastic unloading wave form propagates unchanged. In the former case, then, the plastic front is reduced by an amount

$$n\Delta = 2c_1 n\Delta'/(c_0+c_1),$$

there is a total reflected elastic loading wave amplitude

$$n\Delta'' = (c_0-c_1)\, n\Delta'(c_0+c_1),$$

and spread over the interaction region are n strain discontinuities amounting to a total permanent strain change $-2c_1 n\Delta'(1/c_1^2-1/c_0^2)/\rho_i(c_0+c_1)$.

This sequence may be plotted on a characteristics diagram in the x-t plane, relating the increments Δ, Δ', Δ'' to the stress profile gradient, at the appropriate level, of the plastic front, elastic unloading front, and reflected elastic loading front, respectively; the symmetry permits extension to the limiting case $n\to\infty$. In this way, the reflected stress-wave profile, and permanent strain distribution, at the end of the interaction may be determined; it is more difficult to extract a description of the situation at a stage during the interaction. The analysis in not presented here since a full continuous solution is derived in the next section; the incremental approach was useful to obtain the correct picture.

5. Continuous solution to previous interaction for uniform elastic and plastic wave velocity

In the previous section, a picture of the interaction mechanism was developed. There is a region $x \geqslant x_1(t)$—the interaction line path—in which a forward plastic wave propagates with uniform velocity c_1, and a region $x \leqslant x_1(t)$ in which elastic waves with uniform velocity c_0 propagate in both directions. The interaction starts at $t = 0$, with the interaction line at

$x_1(0) = 0$, and is completed when one of the two interacting waves is annulled. If the plastic front is annulled, then the remaining elastic unloading wave form propagates unchanged, but the alternative case, when a reduced plastic front is left, is the more interesting. Since the interaction line overtakes the plastic wave and is overtaken by the elastic wave

$$c_1 \leqslant \dot{x}_1(t) \leqslant c_0. \tag{5·1}$$

The assumption of uniform wave velocity allows the stress distribution in both regions to be expressed as a solution to the linear wave equation, which is given in §1; thus

$$x \geqslant x_1(t): \quad \sigma(x,t) = f(x-c_1 t), \tag{5·2}$$

$$x \leqslant x_1(t): \quad \sigma(x,t) = g(x-c_0 t) + h(x+c_0 t). \tag{5·3}$$

The initial stress profiles, described in (3·5) to (3·8), give the conditions

$$\psi \geqslant 0: \quad f(\psi) = F(\psi), \tag{5·4}$$

$$\psi \leqslant 0: \quad g(\psi) + h(\psi) = G(\psi). \tag{5·5}$$

These incorporate the uniform stress regions immediately ahead and behind the interaction. The preceding elastic loading wave and oncoming plastic unloading wave are ignored, since they have no effect on this interaction. If the values of $g(\psi)$ and $h(\psi)$ in the rear uniform region are $g_{Y'}$ and $h_{Y'}$ respectively, then

$$g_{Y'} + h_{Y'} = \sigma_{Y'}. \tag{5·6}$$

$h_{Y'}$ is taken arbitrary, and not made zero, since more symmetrical results are obtained in this way. Ahead of the plastic front, $F(\psi) = \sigma_Y$, the initial yield stress. Applying (5·4) to (5·2) gives immediately

$$x \geqslant x_1(t): \quad \sigma(x,t) = F(x-c_1 t), \tag{5·7}$$

since here $x - c_1 t \geqslant 0$ by (5·1); this stress profile is just the section of plastic front not overtaken at time t. Since $h(x+c_0 t) = h_{Y'}$ in $x \leqslant -c_0 t$, the region beyond the reflected wave front, (5·5) gives

$$\psi \leqslant 0: \quad g(\psi) = G(\psi) - h_{Y'}. \tag{5·8}$$

Stress continuity across the interaction line requires

$$\sigma_1(t) = F[x_1(t) - c_1 t] = g[x_1(t) - c_0 t] + h[x_1(t) + c_0 t], \tag{5·9}$$

where $\sigma_1(t)$ is the stress at $x_1(t)$. Now consider the particle velocity distributions, let v_Y and $v_{Y'}$ be the uniform values ahead of, and behind, the wave system, respectively. The particle velocity at any stress level on the plastic front is obtained by integrating (4·1) directly;

$$x \geqslant x_1(t): \quad v(x,t) = v_Y + \frac{1}{\rho_i c_1}\{F(x-c_1 t) - \sigma_Y\}. \tag{5·10}$$

In the elastic region where there are waves in both directions, the relation (1·18) must be used, since (4·1) was derived only for a wave in one direction; thus

$$\begin{aligned} x \leqslant x_1(t): \quad v(x,t) &= v(x,0) - \frac{1}{\rho_i}\int_0^t \left(\frac{\partial \sigma}{\partial x}\right)_x \mathrm{d}t \\ &= v(x,0) + \frac{1}{\rho_i c_0}\{g(x-c_0 t) - G(x) + h_{Y'}\} \\ &\quad - \frac{1}{\rho_i c_0}\{h(x+c_0 t) - h_{Y'}\}. \end{aligned} \tag{5·11}$$

Applying (4·1) to the initial forward unloading wave gives

$$v(x,0) = v_{Y'} + \frac{1}{\rho_i c_0}\{G(x) - \sigma_{Y'}\}, \tag{5·12}$$

and hence

$$x \leqslant x_1(t): \quad v(x,t) = v_{Y'} + \frac{1}{\rho_i c_0}\{g(x-c_0 t) - g_{Y'}\} - \frac{1}{\rho_i c_0}\{h(x+c_0 t) - h_{Y'}\}. \tag{5·13}$$

It can be seen that this result would be obtained by applying (4·2) to each wave separately and combining the solutions. Now consider the change in particle velocity produced by the passage of the initial plastic loading wave and elastic unloading wave in succession; this is

$$v_{Y'} - v_Y = \frac{1}{\rho_i c_1}(\sigma_m - \sigma_Y) - \frac{1}{\rho_i c_0}(\sigma_m - \sigma_{Y'}). \tag{5·14}$$

Equating (5·10) and (5·13), and using (5·14) to satisfy particle velocity continuity on $x_1(t)$, gives

$$c_0\{\sigma_m - F[x_1(t) - c_1 t]\} = c_1\{\sigma_m - \sigma_{Y'} - g[x_1(t) - c_0 t] + g_{Y'} + h[x_1(t) + c_0 t] - h_{Y'}\}. \tag{5·15}$$

Combining (5·9) and (5·15) produces

$$g[x_1(t) - c_0 t] - g_{Y'} = \sigma_m - \sigma_{Y'} - \frac{c_0 + c_1}{2c_1}\{\sigma_m - F[x_1(t) - c_1 t]\}, \tag{5·16}$$

$$h[x_1(t) + c_0 t] - h_{Y'} = \frac{c_0 - c_1}{2c_1}\{\sigma_m - F[x_1(t) - c_1 t]\}, \tag{5·17}$$

where $g(x-c_0 t) - g_{Y'}$ represents the unloading stress-wave amplitude, and $h(x+c_0 t) - h_{Y'}$ the reflected loading stress-wave amplitude. By (5·1), (5·16) expresses $g(\psi)$ for $\psi \leqslant 0$, and comparing this with the equivalent relation in (5·8) gives

$$G[x_1(t) - c_0 t] = \frac{c_0 + c_1}{2c_1} F[x_1(t) - c_1 t] - \frac{c_0 - c_1}{2c_1}\sigma_m, \tag{5·18}$$

which provides the equation for $x_1(t)$ in terms of the known initial stress-wave profiles; the interaction path is thus determined. (5·17) expresses $h(\psi)$ for $\psi \geqslant 0$, that is, $h(x+c_0 t)$ for $x \geqslant -c_0 t$; and in $x \leqslant -c_0 t$, $h(x+c_0 t) = h_{Y'}$. $g(x-c_0 t)$ in $x \leqslant x_1(t)$, $\leqslant c_0 t$ is given by (5·8). The complete stress distribution for all $t \geqslant 0$ is therefore determined; and the particle velocity distribution is consequently derived from (5·10) and (5·13).

If, at the completion of the interaction, $t = t_f$, the plastic front has been reduced to a maximum stress σ_r, the elastic unloading wave being annulled, then

$$\left.\begin{aligned} F[x_1(t_f) - c_1 t_f] &= \sigma^r, \\ g[x_1(t_f) - c_0 t_f] &= g_{Y'}. \end{aligned}\right\} \tag{5·19}$$

Substituting in (5·16)

$$\sigma_m - \sigma_r = \frac{2c_1}{c_0 + c_1}(\sigma_m - \sigma_{Y'}), \tag{5·20}$$

$$\sigma_r - \sigma_{Y'} = \frac{c_0 - c_1}{c_0 + c_1}(\sigma_m - \sigma_{Y'}). \tag{5·21}$$

Alternatively, if $\sigma_m-\sigma_Y \leqslant 2c_1(\sigma_m-\sigma_{Y'})/(c_0+c_1)$, the plastic loading wave is annulled first. Let the elastic unloading wave front then be reduced down to a stress point σ_u on the initial profile, when $g[x_1(t)-c_0t]-g_{Y'}=\sigma_u-\sigma_{Y'}$, and the stress on the interaction line is σ_Y, so from (5·16)

$$\sigma_m-\sigma_Y=\frac{2c_1}{c_0+c_1}(\sigma_m-\sigma_u). \tag{5·22}$$

By (5·17) and (5·22), the reflected elastic loading wave has amplitude

$$(c_0-c_1)\,(\sigma_m-\sigma_u)/(c_0+c_1).$$

The remaining unloading increment, $\sigma_u-\sigma_{Y'}$, propagates unchanged, now unloading from a stress state σ_Y.

In the former case, the plastic front is reduced in amplitude by an amount little less than the initial elastic unloading increment and the reflected elastic loading wave has comparatively small amplitude. This is seen from (5·20) and (5·21) since $c_0^2/c_1^2\sim 1{\cdot}5$, and therefore $2c_1/(c_0+c_1)\sim 0{\cdot}9$, and $(c_0-c_1)/(c_0+c_1)\sim 0{\cdot}1$.

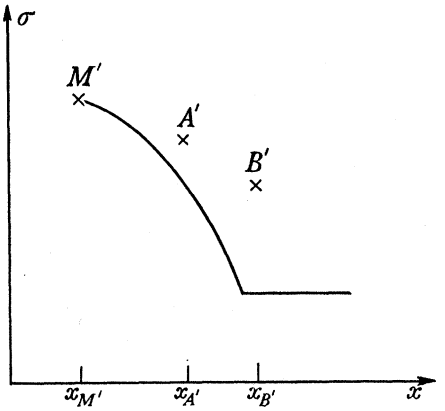

FIGURE 9. Plastic loading stress-wave profile in relation to successive particles, M', A', B', ahead.

To complete the solution, it remains to determine the strain distribution over the region. Let the appropriate uniform strain levels by ϵ_Y and $\epsilon_{Y'}$. Across the plastic front, where the region has a common stress-strain relation, (4·2) can be integrated directly to obtain

$$x\geqslant x_1(t):\quad \epsilon(x,t)=\epsilon_Y+\frac{1}{\rho_i c_1^2}\{F(x-c_1t)-\sigma_Y\}. \tag{5·23}$$

Similarly, combining the strain changes across both initial waves,

$$\epsilon_{Y'}=\epsilon_Y+\frac{1}{\rho_i c_1^2}(\sigma_m-\sigma_Y)-\frac{1}{\rho_i c_0^2}(\sigma_m-\sigma_{Y'}). \tag{5·24}$$

In the elastic region, once the interaction has started, there is a different situation, similar to the series of strain jumps required by the discontinuous solution in §4. A particle $x_{M'}$ (figure 9), loaded to a state M (figure 8) just as the interaction is about to start, will follow an elastic unloading-reloading path MY': a particle $x_{A'}$ (figure 9) a little ahead is only loaded to a state A (figure 8), which is the reduced maximum stress at the time the interaction path reaches $x_{A'}$, and so will follow an elastic unloading-reloading path Aa. Similarly, for successive particles $x_{B'}$.... Since all these elastic paths have the same linear gradient, the elastic

component of the strain increment corresponding to a stress-wave increment is given by (4·2), with $c = c_0$. On applying (4·2) to the interaction between elastic and plastic waves, an additional function of x must be introduced to allow for the different amounts of plastic strain undergone by successive particles. This function represents a permanent strain distribution left over the interaction region when the waves have passed on. Thus

$$x \leqslant x_1(t): \quad \epsilon(x,t) = \epsilon_{Y'} + \frac{1}{\rho_i c_0^2}\{\sigma(x,t) - \sigma_{Y'}\} + \frac{1}{\rho_i c_0^2} k(x). \tag{5·25}$$

The permanent strain distribution, as represented by $k(x)/\rho_i c_0^2$, is determined by satisfying strain continuity across $x_1(t)$, to be consistent with stress continuity there; using (5·23), (5·24) and (5·25):

$$k[x_1(t)] = -\frac{c_0^2 - c_1^2}{c_1^2}\{\sigma_m - F[x_1(t) - c_1 t]\}. \tag{5·26}$$

For all $x \geqslant 0$, $k(x) = 0$, since each particle is unloaded and reloaded along MY'; in $0 \leqslant x \leqslant x_1(t_f)$, $k(x)$ is given by (5·26), decreasing from zero to a value

$$-\frac{c_0^2 - c_1^2}{c_1^2}(\sigma_m - \sigma_r) = -\frac{2(c_0 - c_1)}{c_1}(\sigma_m - \sigma_{Y'}). \tag{5·27}$$

In $x \geqslant x_1(t_f)$, $k(x)$ retains the uniform value $k[_1(t_f)]$ given by (5·27), since all particles are subjected to the same plastic loading.

6. Continuous solution to previous interaction allowing non-uniform plastic wave velocity

It is assumed in this section that shock formation does not start before the interaction is completed. The elastic region, $x \leqslant x_1(t)$, has similar distributions to those of the previous section, namely

$$\sigma(x,t) = g(x - c_0 t) + h(x + c_0 t), \tag{6·1}$$

$$v(x,t) = v_{Y'} + \frac{1}{\rho_i c_0}\{g(x - c_0 t) - g_{Y'} - h(x + c_0 t) + h_{Y'}\}, \tag{6·2}$$

$$\epsilon(x,t) = \epsilon_{Y'} + \frac{1}{\rho_i c_0^2}\{\sigma(x,t) - \sigma_{Y'} + k(x)\}. \tag{6·3}$$

The plastic region $x \geqslant x_1(t)$ is described by the simple wave characteristics solution, since there is a common stress-strain relationship; thus

$$\sigma(x,t) = F[x - t c_1(\sigma)], \tag{6·4}$$

$$v(x,t) = v_Y + \int_{\epsilon Y}^{\epsilon} c_1(\epsilon)\, \mathrm{d}\epsilon, \tag{6·5}$$

$$\epsilon(x,t) = \epsilon[\sigma(x,t)]. \tag{6·6}$$

In addition, the particle velocity change produced by the two initial waves gives

$$v_{Y'} = v_Y + \int_{\epsilon Y}^{\epsilon m} c_1(\epsilon)\, \mathrm{d}\epsilon - \frac{1}{\rho_i c_0}(\sigma_m - \sigma_{Y'}), \tag{6·7}$$

where ϵ_m is the maximum strain behind the initial plastic loading wave.

Defining the stress and strain on $x_1(t)$ as $\sigma_1(t)$ and $\epsilon_1(t)$, respectively, and satisfying continuity of stress, particle velocity, and strain, on $x_1(t)$ gives

$$\sigma_1(t) = F[x_1(t) - tc_1(\sigma)] = g[x_1(t) - c_0 t] + h[x_1(t) + c_0 t], \tag{6·8}$$

$$\sigma_m - \sigma_{Y'} - \rho_i c_0 \int_{\epsilon_1}^{\epsilon_m} c_1(\epsilon)\, \mathrm{d}\epsilon = g[x_1(t) - c_0 t] - g_{Y'} - h[x_1(t) + c_0 t] + h_{Y'}, \tag{6·9}$$

$$\left.\begin{aligned} \epsilon_1(t) &= \epsilon_m - \frac{1}{\rho_i c_0^2}\{\sigma_m - \sigma_1(t) - k[x_1(t)]\}, \\ &= \epsilon[\sigma_1(t)]. \end{aligned}\right\} \tag{6·10}$$

Combining (6·8) and (6·9):

$$g[x_1(t) - c_0 t] - g_{Y'} = \frac{1}{2}\left\{\sigma_m + \sigma_1(t) - 2\sigma_{Y'} - \rho_i c_0 \int_{\epsilon_1}^{\epsilon_m} c_1(\epsilon)\, \mathrm{d}\epsilon\right\}, \tag{6·11}$$

$$h[x_1(t) + c_0 t] - h_{Y'} = \frac{1}{2}\left\{\rho_i c_0 \int_{\epsilon_1}^{\epsilon_m} c_1(\epsilon)\, \mathrm{d}\epsilon - \sigma_m + \sigma_1(t)\right\}. \tag{6·12}$$

Comparing (6·11) with the equivalent expression for $g(\psi)$ in $\psi \leqslant 0$, (5·8), given by the initial conditions:

$$\left.\begin{aligned} G[x_1(t) - c_0 t] &= \frac{1}{2}\left\{\sigma_m + \sigma_1(t) - \rho_i c_0 \int_{\epsilon_1}^{\epsilon_m} c_1(\epsilon)\, \mathrm{d}\epsilon\right\}, \\ &= \sigma_u[\sigma_1(t)], \quad \text{say.} \end{aligned}\right\} \tag{6·13}$$

(6·11) and (6·12) can be rewritten as

$$g[x_1(t) - c_0 t] - g_{Y'} = \sigma_u(\sigma_1) - \sigma_{Y'}, \tag{6·14}$$

$$h[x_1(t) + c_0 t] - h_{Y'} = \sigma_1(t) - \sigma_u(\sigma_1). \tag{6·15}$$

Inverting (6·8) and (6·13)

$$x_1(t) = tc_1[\sigma_1(t)] + \mathscr{F}[\sigma_1(t)], \tag{6·16}$$

$$x_1(t) = c_0 t + \mathscr{G}[\sigma_u(\sigma_1)], \tag{6·17}$$

from which the time t, when the interaction stress level is $\sigma_1(t)$, is given by

$$t\{c_0 - c_1(\sigma)\} = \mathscr{F}(\sigma_1) - \mathscr{G}(\sigma_u). \tag{6·18}$$

This determines $t(\sigma_1)$, and substituting in either (6·16) or (6·17) gives $x_1(t)$. Also, $h(x + c_0 t)$ for $x \geqslant -c_0 t$ is given by (6·15), and $g(x - c_0 t)$ for $x \leqslant x_1(t)$, $\leqslant c_0 t$ by (6·14) or the equivalent initial condition

$$\psi \leqslant 0: \quad g(\psi) = G(\psi) - h_{Y'}. \tag{6·19}$$

The elastic unloading wave is annulled when $\sigma_u(\sigma_1)$ decreases to $\sigma_{Y'}$, by (6·14). If this is at time t_f, and the plastic front is then reduced to a maximum stress σ_r,

$$\sigma_u(\sigma_r) = \sigma_{Y'}. \tag{6·20}$$

Alternatively, if the plastic front is annulled first, the remaining unloading increment propagates unchanged.

To complete the solution, the permanent strain distribution, with properties as before, is derived from (6·10) as

$$k[x_1(t)] = -\{\rho_i c_0^2[\epsilon_m - \epsilon_1(t)] - [\sigma_m - \sigma_1(t)]\}. \tag{6·21}$$

7. Further interactions in the system

The primary unloading interaction just solved produces a reflected elastic loading wave which will meet the oncoming plastic unloading wave. The solution to this secondary interaction is now obtained, but the detailed analysis is not presented since it follows the lines of the previous solution. Only the case of constant elastic and plastic wave velocity is given, and it can be seen from the previous sections that a small variation in $c_1(\epsilon)$ has no marked effect on the resulting wave amplitudes. Since the plastic wave is unloading, the tendency is to spread out and not to form a shock.

The material through which the waves are propagating has previously been subjected to plastic deformation and care must be taken in selecting the correct elastic stress-strain paths which various particles follow during the interation; these are illustrated in figure 10. It is assumed that the region does not overlap the primary interaction region (though if this were the case, the function $k(x)$ should be incorporated in the strain expressions), and that the

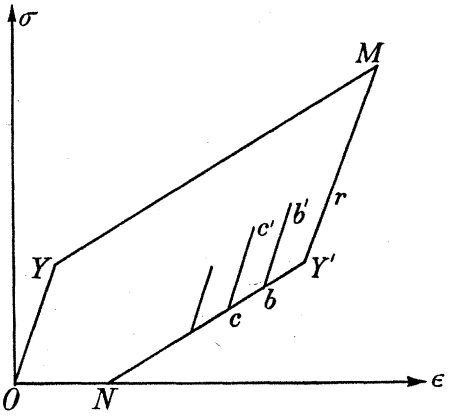

Figure 10. Elastic reloading paths, $Y'r$, bb', ... after different amounts of reverse yielding.

outer regions are uniform. The state behind the plastic unloading wave is represented by N, that behind the elastic loading wave by r, and that between the approaching waves by Y', shown in figure 10. The stress-wave profiles at the start of the interaction are shown in figure 12.

If we consider each wave front as a series of step increments, then the interaction between a plastic unloading and approaching elastic loading increment, illustrated in figure 11, needs analyzing. If the plastic increment is Δ' and the elastic increment is Δ, there results an elastic unloading increment, $(c_0+c_1)\,\Delta'/2c_1$, moving back into the elastic region, and an elastic loading increment, $\Delta-(c_0-c_1)\,\Delta'/2c_1$, moving towards the next plastic step. It is required that the elastic unloading increment has amplitude less than that of the incident elastic loading increment, here $\Delta'\leqslant 2c_1\Delta/(c_0+c_1)$, since unloading beyond the previous yield point, represented by Y' in figure 10, for the case of the first elementary interaction, is no longer elastic. That is, further unloading beyond rY' follows the reverse yield path $Y'N$. Similarly, for subsequent interactions, unloading beyond $b'b$ follows bN, etc. As before, there is a small strain jump created at the interaction line for each interaction involving a plastic increment, the elastic reloading for successive particles following the respective paths $Y'r$, bb', cc' .... Building up the wavelet pattern in this way shows that there are two regions

throughout the interaction, the one to the right containing elastic waves in both directions, and the one to the left containing a plastic wave moving in the positive direction only (towards the right).

Choosing a new x-t origin to represent the start of the interaction, then the initial conditions can be represented by

$$\left.\begin{aligned} x\leqslant 0: &\quad \sigma = G(x),\\ 0\leqslant\sigma\leqslant\sigma_{Y'}: &\quad x = \mathscr{G}(\sigma),\end{aligned}\right\} \tag{7·1}$$

$$\left.\begin{aligned} x\geqslant 0: &\quad \sigma = H(x),\\ \sigma_{Y'}\leqslant\sigma\leqslant\sigma_r: &\quad x = \mathscr{H}(\sigma),\end{aligned}\right\} \tag{7·2}$$

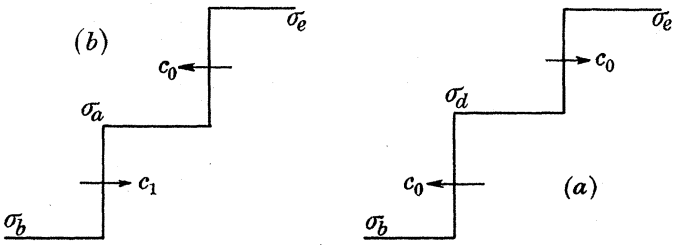

FIGURE 11. Situation before (b) and after (a) interaction between an elastic loading and a plastic unloading increment.

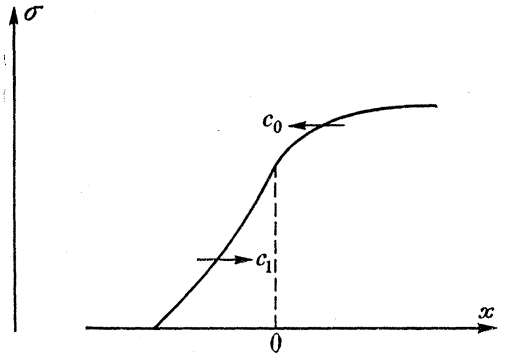

FIGURE 12. Stress-wave profile at start of second interaction.

where the functions $G(x)$, $H(x)$ are different from those of the previous sections, although $H(x)$ differs only by a displacement of the x origin. These are illustrated in figure 12. The wave pattern already described is expressed by

$$x\leqslant x_1(t): \quad \sigma = G(x-c_1t), \tag{7·3}$$

$$x\geqslant x_1(t): \quad \sigma = f(x-c_0t)+h(x+c_0t), \tag{7·4}$$

where the initial state is satisfied by (7·3). Let f_r and h_r be the values of $f(x-c_0t)$ and $h(x+c_0t)$ in the uniform loaded region. The particle velocity distributions in the two regions are given by

$$x\leqslant x_1(t): \quad v(x,t) = v_r+\frac{1}{\rho_ic_0}\{\sigma_r-\sigma_{Y'}\}-\frac{1}{\rho_ic_1}\sigma_{Y'}+\frac{1}{\rho_ic_1}G(x-c_1t), \tag{7·5}$$

$$x\geqslant x_1(t): \quad v(x,t) = v_r+\frac{1}{\rho_ic_0}\{h_r-h(x+c_0t)-f_r+f(x-c_0t)\}. \tag{7·6}$$

Satisfying continuity of stress and particle velocity on the interaction line, $x_1(t)$, gives

$$f_r - f[x_1(t) - c_0 t] = \frac{c_0 + c_1}{2c_1}\{\sigma_{Y'} - G[x_1(t) - c_1 t]\}, \tag{7·7}$$

$$h_r - h[x_1(t) + c_0 t] = \sigma_r - \sigma_{Y'} - \frac{c_0 - c_1}{2c_1}\{\sigma_{Y'} - G[x_1(t) - c_1 t]\}. \tag{7·8}$$

$f(x - c_0 t)$ is determined for $x \leqslant c_0 t$ by (7·7), and ahead it has the uniform value f_r, while equating the expression $h(\psi)$ for $\psi \geqslant 0$ given by (7·8) with the known equivalent initial condition gives

$$H[x_1(t) + c_0 t] - \sigma_{Y'} = \frac{c_0 - c_1}{2c_1}\{\sigma_r - G[x_1(t) - c_1 t]\}, \tag{7·9}$$

which is an equation for $x_1(t)$.

The stress and particle velocity distributions are now determined, and it remains to find the strain distributions. The region $x \leqslant x_1(t)$ is governed by a single stress-strain relation $Y'N$ in figure 10, while successive particles of the elastic region $x \geqslant x_1(t)$ follow different paths $Y'r$, bb', cc', etc., as the interaction proceeds. This situation is expressed by

$$x \leqslant x_1(t): \quad \epsilon(x, t) = \epsilon_N + \frac{1}{\rho_i c_1^2} G(x - c_1 t), \tag{7·10}$$

$$x \geqslant x_1(t): \quad \epsilon(x, t) = \epsilon_r + \frac{1}{\rho_i c_0^2}\{\sigma(x, t) - \sigma_r + k_2(x)\}, \tag{7·11}$$

where ϵ_N and ϵ_r are the strains in the respective uniform regions, related by the strain changes across the initial waves, and $k_2(x)$ represents the permanent-strain distribution over the interaction region. Strain continuity on $x_1(t)$ gives

$$k_2[x_1(t)] = -\frac{c_0^2 - c_1^2}{c_1^2}\{\sigma_{Y'} - G[x_1(t) - c_1 t]\}, \tag{7·12}$$

which determines this permanent strain distribution. There are now two of these distributions in the block, which may overlap.

Depending on the ratio of the initial wave amplitudes, the plastic unloading wave may be completely annulled, in which case an elastic loading wave travels back to the free surface of the block, or the plastic wave is merely reduced. In both cases, an elastic unloading wave propagates to the right, following the original loading front. This secondary interaction also is illustrated in figure 5, showing the latter case. The situation here is determined by the ratio of the component amplitudes of the original applied pulse, and above a moderate value of σ_m, the case in which the plastic unloading wave is not annulled results. But then the elastic unloading wave propagated to the right overtakes the primary plastic loading front (now reduced) and interacts as before, so that a further reflected elastic loading wave approaches the oncoming reduced plastic unloading wave—and so on. At some stage, after the plastic unloading wave is annulled and all elastic loading increments moving to the left are reflected from the free surface as unloading waves, the reduced plastic loading front will be followed by a total elastic unloading wave such that the ultimate interaction annuls the plastic front. If, in the primary interaction, the plastic loading front was annulled, then the resulting amplitudes would be such that the plastic unloading wave is annulled by the secondary interaction. The final situation is that an elastic wave loading up to yield, σ_Y, is

followed by a sequence of elastic unloading waves with total amplitude σ_Y. This result is expected, since a finite amount of energy is imparted to the block by the applied pulse, and a plastic wave is continually dissipating energy.

III. SHOCK-WAVE FORMATION AND PROPAGATION WITH INTERACTION SOLUTIONS

8. Propagation conditions

The plastic loading stress-strain curve derived in § 2 was shown to be concave upwards, and hence the wave velocity is an increasing function of stress. Assuming no interference by a following unloading wave, the plastic unloading wave form is determined by the 'simple wave' characteristics solution from the initial profile; each stress increment propagates with a constant velocity $c_1(\sigma)$. Since increments at higher stresses propagate faster, the stress-wave profile at each level becomes continually steeper, until eventually the profile becomes vertical at some stress point. The continuous solution now predicts more than one value of stress (particle velocity, and strain) for a single particle, and so is no longer valid. By analogy with the corresponding situation in fluid dynamics, it is expected that the plastic loading front propagates as a plane shock wave beyond this stage. This is a very short pulse across which the stress, strain, and particle velocity, change rapidly.

The approximation, usual in fluid dynamics, is made of considering this narrow shock-wave region as a discontinuity of zero width with the appropriate jumps in stress and strain; it is shown that the particle velocity jump predicted by the propagation conditions corresponds almost exactly to the true continuous increase. The manner in which the continuous loading front breaks down, and the determination of the subsequent shock front paths, are also treated in this section.

Let the shock front have velocity D in space, and let it transform material from a state 0 to a state 1. The velocity of material relative to the shock, q, is given by

$$q = v - D. \tag{8·1}$$

The equations of mass and momentum flow across the shock are

$$\rho_1 q_1 = \rho_0 q_0, \tag{8·2}$$

$$\sigma_1 - \sigma_0 = \rho_0 q_0^2 - \rho_1 q_1^2. \tag{8·3}$$

Combining these produces

$$\left.\begin{aligned} q_0^2 &= \frac{\rho_1(\sigma_1-\sigma_0)}{\rho_0(\rho_1-\rho_0)}, \\ q_1^2 &= \frac{\rho_0(\sigma_1-\sigma_0)}{\rho_1(\rho_1-\rho_0)}. \end{aligned}\right\} \tag{8·4}$$

If U is the internal energy per unit mass, then energy flow across the shock satisfies

$$\rho_1 q_1 U_1 - \rho_0 q_0 U_0 = \sigma_0 q_0 - \sigma_1 q_1 + \tfrac{1}{2}\rho_0 q_0^3 - \tfrac{1}{2}\rho_1 q_1^3. \tag{8·5}$$

Substituting for the q's from (8·4),

$$\begin{aligned} U_1 - U_0 &= \frac{\sigma_0}{\rho_0} - \frac{\sigma_1}{\rho_1} + \frac{1}{2}\frac{\rho_0+\rho_1}{\rho_0\rho_1}(\sigma_1-\sigma_0), \\ &= \tfrac{1}{2}(\sigma_1+\sigma_0)(V_0-V_1). \end{aligned} \tag{8·6}$$

Substituting for ρ in terms of ϵ, (8·4) becomes

$$-q_0 = (1-\epsilon_0)\left\{\frac{\sigma_1-\sigma_0}{\rho_i(\epsilon_1-\epsilon_0)}\right\}^{\frac{1}{2}}, \tag{8·7}$$

and

$$-q_1 = (1-\epsilon_1)\left\{\frac{\sigma_1-\sigma_0}{\rho_i(\epsilon_1-\epsilon_0)}\right\}^{\frac{1}{2}}. \tag{8·8}$$

Define the particle velocity jump across the shock as $\bar{v}_s$, then

$$\bar{v}_s = v_1 - v_0 = (\epsilon_1-\epsilon_0)\left\{\frac{\sigma_1-\sigma_0}{\rho_i(\epsilon_1-\epsilon_0)}\right\}^{\frac{1}{2}}. \tag{8·9}$$

Consider the situation reported in the experimental work (Pack *et al.* 1948; Mallory 1955; Walsh & Christian 1955), when the shock has greater velocity than the initial elastic loading wave; the shock then moves into material at rest, so by (8·7)

$$D = -q_0 = \left\{\frac{\sigma_1}{\rho_i\epsilon_1}\right\}^{\frac{1}{2}}. \tag{8·10}$$

Define the straight line joining the states in front of, and behind, the shock, in the stress-strain plane, as the shock chord. For the case described by (8·10), the shock chord is steeper than the initial elastic loading line, and hence the continuous plastic wave velocity at (ϵ_1, σ_1)

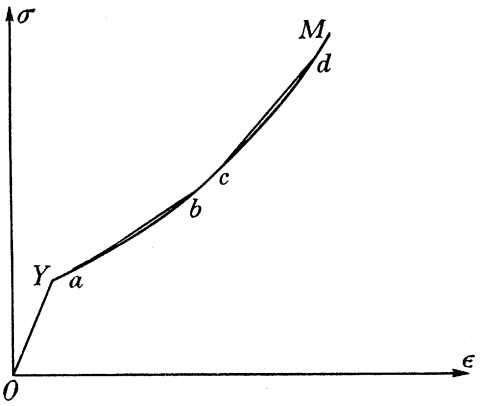

FIGURE 13. Plastic loading stress-strain curve with fitted shock chords, *ab*, *cd*.

must also be greater than the initial elastic loading wave velocity. This is seen from figure 13 which shows that the shock chord gradient is less than that of the continuous plastic stress-strain curve at the corresponding maximum stress point. As shown in § 2, the elastic unloading path from the state (ϵ_1, σ_1) is steeper again.

The particle velocity jump, $\bar{v}_s$, predicted by the shock conditions must be compared with the actual particle velocity change across the original plastic loading wave, $\bar{v}_c$.

$$\bar{v}_c = \int_{\epsilon_0}^{\epsilon_1} c_1(\epsilon)\,\mathrm{d}\epsilon. \tag{8·11}$$

The plastic loading stress-strain relation is given by

$$\frac{\mathrm{d}\sigma}{\mathrm{d}\epsilon} = \tfrac{1}{3}\alpha\beta\{1 + d_1\epsilon + d_2\epsilon^2 + d_3\epsilon^3 + \ldots\}, \tag{8·12}$$

where d_1, d_2, d_3 may be deduced from (2·32). Thus

$$\sigma-\sigma_Y=\tfrac{1}{3}\alpha\beta[\epsilon+\tfrac{1}{2}d_1\epsilon^2+\tfrac{1}{3}d_2\epsilon^3+\ldots]_{\epsilon_Y}^{\epsilon}, \tag{8·13}$$

and

$$c_1(\epsilon)=\left\{\frac{\alpha\beta}{3\rho_i}\right\}^{\frac{1}{2}}\{1+\tfrac{1}{2}d_1\epsilon+(\tfrac{1}{2}d_2-\tfrac{1}{8}d_1^2)\,\epsilon^2+\ldots\}. \tag{8·14}$$

Hence, from (8·11),

$$\bar{v}_c=\left\{\frac{\alpha\beta}{3\rho_i}\right\}^{\frac{1}{2}}[\epsilon+\tfrac{1}{4}d_1\epsilon^2+\tfrac{1}{3}(\tfrac{1}{2}d_2-\tfrac{1}{8}d_1^2)\epsilon^3+\ldots]_{\epsilon_1}^{\epsilon_0}, \tag{8·15}$$

and, using (8·13),

$$\frac{\sigma_1-\sigma_0}{\epsilon_1-\epsilon_0}=\tfrac{1}{3}\alpha\beta\{1+\tfrac{1}{2}d_1(\epsilon_1+\epsilon_0)+\tfrac{1}{3}d_2(\epsilon_1^2+\epsilon_1\epsilon_0+\epsilon_0^2)+\ldots\}, \tag{8·16}$$

from which

$$\left\{\frac{\sigma_1-\sigma_0}{\rho_i(\epsilon_1-\epsilon_0)}\right\}^{\frac{1}{2}}=\left\{\frac{\alpha\beta}{3\rho_i}\right\}^{\frac{1}{2}}\{1+\tfrac{1}{4}d_1(\epsilon_1+\epsilon_0)+\tfrac{1}{6}d_2(\epsilon_1^2+\epsilon_1\epsilon_0+\epsilon_0^2)-\tfrac{1}{32}d_1^2(\epsilon_1+\epsilon_0)^2+\ldots\}, \tag{8·17}$$

and therefore

$$\bar{v}_s=\left\{\frac{\alpha\beta}{3\rho_i}\right\}^{\frac{1}{2}}\{(\epsilon_1-\epsilon_0)+\tfrac{1}{4}d_1(\epsilon_1^2-\epsilon_0^2)+\tfrac{1}{6}d_2(\epsilon_1^3-\epsilon_0^3)-\tfrac{1}{32}d_1^2(\epsilon_1-\epsilon_0)\,(\epsilon_1+\epsilon_0)^2+\ldots\}. \tag{8·18}$$

Hence, neglecting terms of order ϵ^4 upwards, (8·15) and (8·18) give

$$\bar{v}_s-\bar{v}_c=\left\{\frac{\alpha\beta}{3\rho_i}\right\}^{\frac{1}{2}}\left\{\frac{d_1^2(\epsilon_1-\epsilon_0)^3}{96}\right\}, \tag{8·19}$$

and

$$\frac{\bar{v}_s-\bar{v}_c}{\bar{v}_c}=\frac{d_1^2(\epsilon_1-\epsilon_0)^2}{96}. \tag{8·20}$$

Now $d_1=(6+\beta)/3$, $\sim 5{\cdot}5$ for aluminium; allowing a strain increase of order 0·1, the percentage error represented by (8·20) is of order 0·3. The discontinuous shock front therefore provides a very close approximation to the particle velocity change across the continuous wave. This will hold for all metals for which β is not of greater order than 10.

It is now shown that the shock change is not adiabatic, but that there is a finite amount of heat energy dissipated as the shock passes through the material. Let the irreversible energy dissipated per unit mass in a small compression $\mathrm{d}\epsilon$ be $\mathrm{d}Q$ then

$$\mathrm{d}Q=\mathrm{d}U-\mathrm{d}W, \tag{8·21}$$

where $\mathrm{d}U$ is the increase in internal energy, and $\mathrm{d}W$ the work done by the applied field, per unit mass. Taylor & Farren (1925) and Hawkyard & Freeman (1951) have shown that less than 15 % of the plastic work goes into producing structural changes, and so the heat dissipation per unit mass represents more than 85 % of $\mathrm{d}Q$. On integrating over the full compression, the increase of U is known from (8·6), and is

$$U_1-U_0=(1/2\rho_i)\,(\sigma_1+\sigma_0)\,(\epsilon_1-\epsilon_0). \tag{8·22}$$

The work increment per unit mass, noting that there is no lateral strain and that engineering stress and strain are used, is

$$\mathrm{d}W=(1/\rho_i)\,\sigma\,\mathrm{d}\epsilon. \tag{8·23}$$

The total applied work, ignoring the factor $1/\rho_i$, is therefore the area under the corresponding stress-strain curve, and the area under the shock chord represents the increase

in U; the difference represents Q, the energy dissipated, as pointed out by Lee & Tupper (1954). The stress-strain relation through the shock is not known, and is likely to differ from the adiabatic relation, but the latter is now used in order to estimate the applied work. It is probable that this approximation underestimates the area difference, Q, but the reverse tendency is also present since isothermal data are used as an approximation for the adiabatic path, so exaggerating the curvature; reference to figure 13 is helpful for comparing the areas. From (8·13)

$$\tfrac{1}{2}(\sigma_1+\sigma_0) = \{\sigma_Y-\tfrac{1}{3}\alpha\beta[\epsilon_Y+\tfrac{1}{2}d_1\epsilon_Y^2+\ldots]\}+\tfrac{1}{3}\alpha\beta\{\tfrac{1}{2}(\epsilon_1+\epsilon_0)+\tfrac{1}{4}d_1(\epsilon_1^2+\epsilon_0^2)+\ldots\}, \tag{8·24}$$

and

$$\int_{\epsilon_0}^{\epsilon_1}\sigma\,\mathrm{d}\epsilon = (\epsilon_1-\epsilon_0)\{\sigma_Y-\tfrac{1}{3}\alpha\beta[\epsilon_Y+\tfrac{1}{2}d_1\epsilon_Y^2+\ldots]\}+\tfrac{1}{3}\alpha\beta\{\tfrac{1}{2}(\epsilon_1^2-\epsilon_0^2)+\tfrac{1}{6}d_1(\epsilon_1^3-\epsilon_0^3)+\ldots\}. \tag{8·25}$$

Hence, neglecting terms of order ϵ^4 upwards,

$$Q = \frac{\alpha\beta}{3\rho_i}\frac{d_1}{12}(\epsilon_1-\epsilon_0)^3. \tag{8·26}$$

Substituting values for aluminium: $\rho_i = 2{\cdot}7\ \mathrm{g/cm^3}$, $C_v = 0{\cdot}9\ \mathrm{J\,g^{-1}\,°C^{-1}}$, $\alpha = 20\times10^{10}\ \mathrm{dyn/cm^2}$, $\beta = 10$, (8·26) gives

$$Q\sim13C_v\{10(\epsilon_1-\epsilon_0)\}^3, \tag{8·27}$$

when, for $(\epsilon_1-\epsilon_0) = 0{\cdot}1$ and $0{\cdot}05$, $Q\sim13C_v$ and $1{\cdot}5C_v$, respectively.

The above analysis holds for any set of coefficients d_1, d_2, ..., and so if the actual stress-strain relation is represented by a power series such that d_1 is not much greater than the above value, that is, β, which represents the curvature, is not much larger, then a similar result will be obtained. It appears that for $(\epsilon_1-\epsilon_0)<0{\cdot}05$, the shock change is virtually adiabatic, and the material behind the shock will satisfy the original adiabatic stress-strain relation; this is the assumption made in §9 to treat the unloading of a shock. The approximation becomes poorer with increasing strain jump.

The plastic loading wave form, as derived by the simple-wave characteristics solution, becomes physically unsound when the stress (or strain) profile becomes vertical; which may occur first at any stress level on the plastic wave front. If $\mathscr{F}(\sigma)$ and $\phi(\epsilon)$ represent the initial stress and strain profiles respectively, then those at a subsequent time t, as predicted by the characteristics solution, are represented by

$$\left.\begin{aligned} x &= \mathscr{F}(\sigma)+tc_1(\sigma),\\ x &= \phi(\epsilon)+tc_1(\epsilon). \end{aligned}\right\} \tag{8·28}$$

Initial breakdown takes place as soon as

$$\left.\begin{aligned} \mathscr{F}'(\sigma)+tc_1'(\sigma) &= 0,\\ \phi'(\epsilon)+tc_1'(\epsilon) &= 0, \end{aligned}\right\} \tag{8·29}$$

which is at a time t_s given by

$$t_s = \left\{-\frac{\mathscr{F}'(\sigma)}{c_1'(\sigma)}\right\}_{\text{min.}} = \left\{-\frac{\phi'(\epsilon)}{c_1'(\epsilon)}\right\}_{\text{min.}}. \tag{8·30}$$

An elementary shock is formed, represented by a chord across the adiabatic curve, *ab* say, in figure 13. Further breakdown may occur separately at another stress level, corresponding to a shock chord *cd* say. The continuous plastic wave continuously overtakes a shock ahead,

which is clear from (8·8) and comparison of the shock-chord gradient with that of the adiabatic loading curve at the rear stress point; for example, at b in figure 13. The shock is thus gradually built up from the rear; a reflected disturbance incorporated to satisfy velocity continuity at the overtaking line is negligible, and will be ignored. This is because the particle velocity jump across a shock front is very closely equal to the corresponding increase across the continuous plastic loading wave. If separate breakdown, cd, occurs behind, the preceding shock, ab, is built up by the above process until the stress point b coincides with the lower stress point c of the following shock; the latter clearly overtakes as is seen by comparison of the two shock-chord gradients. On interaction, the two shocks combine, and as before, the reflected disturbance is negligible. It is not certain that a shock propagates into the material ahead faster than a continuous plastic wave there, because of the factor $(1-\epsilon_0)$ in the expression (8·7) for $-q_0$, but this preceding wave-form must itself break down, and a total shock is formed as above.

It is now required to trace the shock-front pattern so developed. This can be achieved with simplicity by consideration of mass conservation; the idea is due to Lighthill (1956). A shock front is introduced to replace a section of the continuous wave form which has become physically unsound; both solutions satisfy mass conservation. If X is the Eulerian co-ordinate defining a point in space, then mass conservation is expressed by

$$\left(\frac{\partial X}{\partial x}\right)_t = \frac{\rho_i}{\rho}. \tag{8·31}$$

At any particular instant, integrate over a fixed region of space $\langle X_0, X_1\rangle$ which encloses the plastic wave-form but excludes other disturbances; thus

$$\int \mathrm{d}x/\rho = \text{constant}. \tag{8·32}$$

Substituting for ρ in terms of ϵ,

$$\int (1-\epsilon)\,\mathrm{d}x = \text{constant}, \tag{8·33}$$

and since $\int \mathrm{d}x$ is constant, being the initial length of material enclosed in $\langle X_0, X_1\rangle$ at that instant, (8·33) becomes

$$\int \epsilon\,\mathrm{d}x = \text{constant}. \tag{8·34}$$

That is, the change in length of material enclosed in the plastic wave form is the same for all solutions satisfying conservation of mass; introduction of a shock front does not influence material outside the plastic wave form.

This result is best applied in terms of strain profile, figure 14 shows the strain profile, subsequent to breakdown, as determined by the characteristics solution; in the situation represented, two distinct shock fronts are required to replace corresponding sections of the continuous profile. Equation (8·34) indicates that the area under the strain profile is identical for both solutions; this may be interpreted as area A_1 = area A_2, and area B_1 = area B_2. The formation of a single stable shock occurs when the upper loop extends sufficiently over the lower one for a single shock front to satisfy area (A_1+B_1) = area (A_2+B_2). If 0 and 1 represent states ahead of, and behind, the single shock, the general result is expressed by

$$\int_{\epsilon_0}^{\epsilon_1} \{\phi(\epsilon) + tc_1(\epsilon) - x_s(t)\}\,\mathrm{d}\epsilon = 0, \tag{8·35}$$

where $x_s(t)$ is the shock-front path given by

$$\left.\begin{aligned} x_s(t) &= \phi(\epsilon_0) + tc_1(\epsilon_0), \\ &= \phi(\epsilon_1) + tc_1(\epsilon_1). \end{aligned}\right\} \tag{8·36}$$

This result may be expressed in terms of stress profile by

$$\int_{\epsilon_0}^{\epsilon_1} \{\mathscr{F}(\sigma) + tc_1(\sigma) - x_s(t)\}\,\mathrm{d}\epsilon = 0, \tag{8·37}$$

$$\left.\begin{aligned} x_s(t) &= \mathscr{F}(\sigma_0) + tc_1(\sigma_0), \\ &= \mathscr{F}(\sigma_1) + tc_1(\sigma_1), \end{aligned}\right\} \tag{8·38}$$

together with the known plastic loading stress-strain relation $\sigma(\epsilon)$.

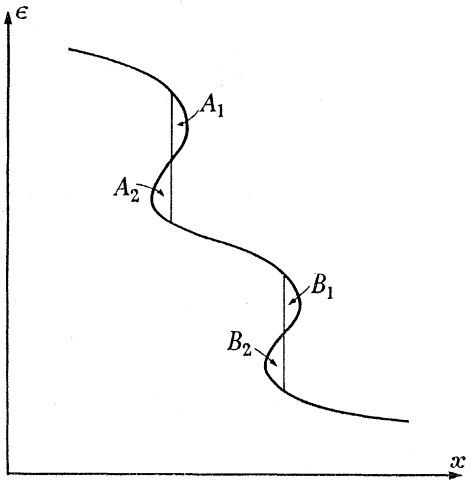

FIGURE 14. Continuous plastic loading strain profile subsequent to breakdown, with fitted shock fronts.

9. ELASTIC UNLOADING OF A PLASTIC FRONT DURING SHOCK FORMATION

Earlier, the interaction between the plastic loading front and the overtaking elastic unloading wave has been solved for initial wave profiles such that the interaction is completed before the breakdown of the plastic front into shock begins. Section 8 has dealt with shock formation across a continuous plastic loading wave front; this can be applied to the reduced plastic loading wave which results from the above interaction. The general problem, when breakdown occurs during the interaction, will now be considered. The first stage is to take the case of a pure shock front overtaken by an elastic unloading wave, and then it is shown how this solution can be combined with that for the continuous-wave interaction, together with the shock-path pattern obtained in § 8, to describe fully the behaviour as the unloading wave overtakes the plastic front while it is breaking down.

The shock front, which replaces a corresponding plastic continuous loading front, is assumed not to affect the adiabatic stress-strain relation of material which it passes through; in § 8 it was shown that the shock wave is virtually adiabatic up to quite high strain jumps. The interaction, then, must proceed in similar fashion to that for the case of a continuous plastic front; the loading front is gradually reduced, and elastic loading increments are reflected back; a permanent strain distribution is left in the material as before. The resulting

stress-wave amplitudes were determined solely in terms of the initial stress-wave amplitudes, by applying continuity of stress and particle velocity; replacing the plastic wave by a discontinuous shock front introduces only a negligible difference in the particle velocity change, and hence the new resulting stress-wave amplitudes will be the same. Consequently, the annullment conditions are identical. The difference appears in the interaction path, which now becomes the shock-front path; this depends on the stress jump, which decreases during the unloading.

If we ignore further disturbances which do not influence the interaction, the region ahead of the shock-front path, $x_1(t)$, is uniform (denoted by a suffix Y); that behind contains elastic waves moving in both directions, to the rear of which it is again uniform (denoted by a suffix Y'). Let the initial maximum stress state behind the shock be denoted by a suffix m, then the changes across the initial elastic unloading wave satisfy

$$v_m - v_{Y'} = \frac{1}{\rho_i c_0}(\sigma_m - \sigma_{Y'}), \tag{9·1}$$

$$\epsilon_m - \epsilon_{Y'} = \frac{1}{\rho_i c_0^2}(\sigma_m - \sigma_{Y'}). \tag{9·2}$$

As before, in $x \leqslant x_1(t)$ $$\sigma(x,t) = g(x-c_0t) + h(x+c_0t), \tag{9·3}$$

$$v(x,t) - v_{Y'} = \frac{1}{\rho_i c_0}\{g(x-c_0t) - g_{Y'} - h(x+c_0t) + h_{Y'}\}, \tag{9·4}$$

$$\epsilon(x,t) - \epsilon_{Y'} = \frac{1}{\rho_i c_0^2}\{\sigma(x,t) - \sigma_{Y'} + k(x)\}. \tag{9·5}$$

The state immediately behind the shock front, where the stress is denoted by $\sigma_1(t)$, satisfies the original plastic loading stress-strain relation

$$\sigma_1 = \sigma_1(\epsilon_1). \tag{9·6}$$

The particle velocity jump across the shock was obtained in § 8, and is

$$\left.\begin{aligned} v_1 - v_Y &= (\epsilon_1 - \epsilon_Y)\left\{\frac{\sigma_1 - \sigma_Y}{\rho_i(\epsilon_1 - \epsilon_Y)}\right\}^{\frac{1}{2}}, \\ &= \psi(\sigma_1), \text{ say,} \end{aligned}\right\} \tag{9·7}$$

and in particular $$v_m - v_Y = \psi(\sigma_m). \tag{9·8}$$

Equating the two sets of expressions for stress and particle velocity, (9·3), (9·6) and (9·4), (9·7), respectively, immediately behind the shock, that is, on $x_1(t)$, using (9·1) and (9·8) to eliminate $v_{Y'}$ and v_Y, gives

$$\sigma_1(t) = g[x_1(t) - c_0t] + h[x_1(t) + c_0t], \tag{9·9}$$

and $$\sigma_m - \sigma_{Y'} - g[x_1(t) - c_0t] + g_{Y'} + h[x_1(t) + c_0t] - h_{Y'} = \rho_i c_0\{\psi(\sigma_m) - \psi(\sigma_1)\}, \tag{9·10}$$

which combine to give

$$g[x_1(t) - c_0t] - g_{Y'} = \tfrac{1}{2}\{(\sigma_m - \sigma_{Y'}) + (\sigma_1 - \sigma_{Y'}) - \rho_i c_0[\psi(\sigma_m) - \psi(\sigma_1)]\}, \tag{9·11}$$

$$h[x_1(t) + c_0t] - h_{Y'} = \tfrac{1}{2}\{\rho_i c_0[\psi(\sigma_m) - \psi(\sigma_1)] - (\sigma_m - \sigma_1)\}. \tag{9·12}$$

Once the corresponding $x_1(t)$, $\sigma_1(t)$ are known, then (9·12) gives $h(\xi)$ for $\xi \geqslant x_1(t_0)+c_0t_0$ (where the interaction starts at $t=t_0$); that is, $h(x+c_0t)$ for $x \geqslant x_1(t_0)-c_0(t-t_0)$ as required; behind this region $h(x+c_0t)$ takes the uniform value $h_{Y'}$. From physical considerations $\dot{x}_1(t) \leqslant c_0$, and hence (9·11) gives $g(\xi)$ for $\xi \leqslant x_1(t_0)-c_0t_0$, that is, $g(x-c_0t)$ for $x \leqslant x_1(t_0)+c_0(t-t_0)$. Putting $t=t_0$, an expression is obtained for $g(x-c_0t)$ in $x \leqslant x_1(t_0)$; but this is also defined by the initial conditions

$$\left.\begin{aligned} t=t_0: \quad & \sigma = G(x-c_0t_0), \\ x \leqslant x_1(t_0): \quad & h(x+c_0t_0) = h_{Y'}, \end{aligned}\right\} \tag{9·13}$$

applied to (9·3). Combining the two relations produces

$$\left.\begin{aligned} G[x_1(t)-c_0t] &= \tfrac{1}{2}\{(\sigma_m+\sigma_1)-\rho_ic_0[\psi(\sigma_m)-\psi(\sigma_1)]\}, \\ &= \sigma_u(\sigma_1), \quad \text{say}, \end{aligned}\right\} \tag{9·14}$$

and inverting this relation,

$$\mathscr{G}[\sigma_u(\sigma_1)] = x_1(t)-c_0t. \tag{9·15}$$

The shock-front path $x_1(t)$ is also related to $\sigma_1(t)$ by

$$\dot{x}_1(t) = -q_0(\sigma_1), \tag{9·16}$$

where

$$-q_0(\sigma_1) = (1-\epsilon_0)\left\{\frac{\sigma_1-\sigma_0}{\rho_i(\epsilon_1-\epsilon_0)}\right\}^{\frac{1}{2}} \tag{9·17}$$

is the velocity of the shock relative to the material ahead. Combining (9·15) and (9·16) gives

$$t-t_0 = \int_{\sigma_1}^{\sigma_m} \frac{\mathscr{G}'(\sigma_u)\,\sigma_u'(\sigma_1)}{c_0+q_0(\sigma_1)}\,\mathrm{d}\sigma_1, \tag{9·18}$$

which together with (9·15) determines the corresponding relation $x_1(t)$, $\sigma_1(t)$. As before, the equations (9·11) and (9·12) can be rewritten as

$$\left.\begin{aligned} g[x_1(t)-c_0t]-g_{Y'} &= \sigma_u(\sigma_1)-\sigma_{Y'}, \\ h[x_1(t)+c_0t]-h_{Y'} &= \sigma_1(t)-\sigma_u(\sigma_1). \end{aligned}\right\} \tag{9·19}$$

Further, since $\psi(\sigma_1)$ represents the particle velocity jump, which is equivalent to the corresponding continuous change since the error introduced by the discontinuous shock-front approximation is negligible, the expression obtained for $\sigma_u(\sigma_1)$ in the continuous wave solution can be used; that is

$$\sigma_u(\sigma_1) = \frac{1}{2}\left\{(\sigma_m+\sigma_1)-\rho_ic_0\int_{\epsilon_1}^{\epsilon_m} c_1(\epsilon)\,\mathrm{d}\epsilon\right\}. \tag{9·20}$$

This form is the more advantageous for use later.

Now the $\sigma_1(t)$ relation given by (9·18) is rather unwieldy, but a good approximation can be obtained which readily produces a solution. Throughout the unloading interaction, make

$$\dot{x}_1(t) = -q_0(\sigma_m) = \text{constant}. \tag{9·21}$$

From (8·17),

$$-q_0(\sigma_1) \sim \left\{\frac{\alpha\beta}{3\rho_i}\right\}^{\frac{1}{2}}(1-\epsilon_0)\left\{1+\frac{6+\beta}{12}(\epsilon_0+\epsilon_1)\right\}, \tag{9·22}$$

and hence

$$\frac{q_0(\sigma_m)-q_0(\sigma_1)}{q_0(\sigma_m)} \sim \frac{6+\beta}{12}(\epsilon_m-\epsilon_1). \tag{9·23}$$

Now the maximum possible decrease in stress on the plastic front is

$$(\sigma_m-\sigma_{Y'})\,2c_1(\sigma_m)/[c_0+c_1(\sigma_m)],$$

and so the maximum strain decrease is of order

$$2c_1(\sigma_m)\left[\int_{\sigma_{Y'}}^{\sigma_m} \mathrm{d}\sigma/\rho_i c_1^2(\sigma_m)\right]\Big/[c_0+c_1(\sigma_m)].$$

This is equal to

$$\frac{2c_0^2}{c_1^2(\sigma_m)}\,\frac{2c_1(\sigma_m)}{c_0+c_1(\sigma_m)}\int_{\sigma_{Y'}}^{\sigma_m}\frac{\mathrm{d}\sigma}{\rho_i c_0^2}=\frac{2c_0^2}{c_1(\sigma_m)\,[c_0+c_1(\sigma_m)]}\,(\epsilon_m-\epsilon_{Y'}).$$

But $c_0^2/c_1^2=1+4\mu/3k=3(1-\nu)/(1+\nu)\sim\frac{3}{2}$, which gives $2c_1/(c_0+c_1)\sim 0{\cdot}9$, and so the maximum strain decrease $\sim 1{\cdot}4\ (\epsilon_m-\epsilon_{Y'})\sim 1{\cdot}4\times 0{\cdot}012$ (since $\epsilon_m-\epsilon_{Y'}$ is roughly twice the initial yield strain), $\sim 0{\cdot}017$. Hence

$$\frac{q_0(\sigma_m)-q_0(\sigma_1)}{q_0(\sigma_m)}<\frac{6+\beta}{12}\times 0{\cdot}017. \tag{9·24}$$

For $\beta\sim 10$ (aluminium), (9·24) represents a percentage error of order 2·3; the error increases from zero as σ_1 is reduced from σ_m. If we suppose that $q_0(\sigma_1)$ varies linearly with time during the unloading, then the error in the length covered by $x_1(t)$ during the interaction, introduced by this approximation, will be at most 1·2 %. Applying (9·21) to (9·15) gives

$$\mathscr{G}[\sigma_u(\sigma_1)]=x_1(t_0)+[t-t_0]\,[-q_0(\sigma_m)]-c_0 t, \tag{9·25}$$

which is an expression for $\sigma_1(t)$; the corresponding $x_1(t)$ is given by (9·21).

It remains to derive the permanent strain distribution produced over the interaction region. Using (9·2) and (9·5), the strain immediately behind the shock —$\epsilon_1(t)$ on $x_1(t)$— is given by

$$\epsilon_m-\epsilon_1(t)=\frac{1}{\rho_i c_0^2}\{\sigma_m-\sigma_1(t)+k[x_1(t)]\}, \tag{9·26}$$

which combined with the known relations $\sigma_1(\epsilon_1)$, $x_1(t)$, and $\sigma_1(t)$, provides an expression for $k(x)$. As before, $k(x)$ will be zero at $x_1(t_0)$, and decrease with increase of x becoming uniform beyond the interaction region.

The interaction is completed when $g(x-c_0t)$ takes the value $g_{Y'}$ in $x\leqslant x_1(t)$ (that is, when σ_u is reduced to $\sigma_{Y'}$), unless the shock is completely unloaded first, when the remaining unloading section propagates unchanged.

To consider the most general situation, suppose the plastic loading front breaks down in different sections to form a series of shocks with paths $x_{s_1}(t)$, $x_{s_2}(t)$, ..., which are determined by the result given in §8. Figure 15 shows a case with two sections of the continuous plastic front replaced by shocks. Eventually a single stable shock front is formed. If the elastic wave overtakes the plastic front in such a state, then the interaction proceeds as described in §6, until such time as the continuous plastic profile behind the first shock is unloaded; that is, $x_1(t)=x_{s_1}(t)$. The shock path $x_{s_1}(t)$ is clearly unaffected by the unloading interaction taking place in the region behind, which can be proved by applying the appropriate analysis in §8 to a section of material which excludes the interaction region. This shock is now unloaded as described in the last section, and then the unloading continues through the next section of continuous profile until the interaction path coincides with the second shock-front path,

which has not been affected by the interactions taking place behind. The interaction proceeds in this manner until the elastic unloading wave is annulled (assuming that the total plastic front is not completely unloaded first); the final stress-wave amplitudes depend only on the initial wave amplitudes, and are not influenced by shock formation across sections of the continuous plastic front. Throughout, the region behind the interaction line contains elastic waves in both directions, and so the stress distribution is described by

$$\sigma(x,t) = g(x-c_0t)+h(x+c_0t), \tag{9·27}$$

where

$$\left.\begin{aligned} g[x_1(t)-c_0t]-g_{Y'} &= \sigma_u(\sigma_1)-\sigma_{Y'},\\ h[x_1(t)+c_0t]-h_{Y'} &= \sigma_1(t)-\sigma_u(\sigma_1),\end{aligned}\right\} \tag{9·28}$$

and

$$\sigma_u(\sigma_1) = \frac{1}{2}\left\{(\sigma_m+\sigma_1)-\rho_ic_0\int_{\epsilon_1}^{\epsilon_m} c_1(\epsilon)\,\mathrm{d}\epsilon\right\}. \tag{9·29}$$

The same equations, (9·28) and (9·29), were derived for both types of interaction. The overall interaction is completed when $\sigma_u(\sigma_1)$ is reduced to $\sigma_{Y'}$, unless the plastic front is annulled

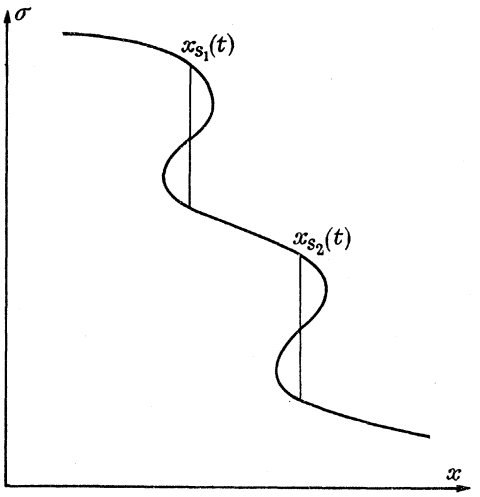

FIGURE 15. Continuous plastic loading stress profile subsequent to breakdown with fitted shock fronts.

first when the remaining section of the elastic unloading wave propagates unchanged. The above equations provide a complete solution once the corresponding relations, $x_1(t)$, $\sigma_1(t)$, are known throughout the interaction. The interaction path, $x_1(t)$, must be followed through the sequence of events described above; when it is moving through a continuous plastic wave front, $x_1(t)$, $\sigma_1(t)$, are determined from the equations (6·17) and (6·18); when it is coinciding with a shock front, they are given by (9·21) and (9·25). The equation (9·14) used to obtain (9·25) is unaltered by the different stress distribution in $x \leqslant x_1(t_p)$, where t_p is the time when the shock unloading starts, since the unloading wave profile in $x \leqslant x_1(t_p)$ at time t_p, to be equated with the expression (9·11), is still given by

$$g(x-c_0t_p)-g_{Y'} = G(x-c_0t_p)-\sigma_{Y'}. \tag{9·30}$$

It can be seen that the whole solution depends on the shock-path pattern $x_{s_1}(t)$, $x_{s_2}(t)$, ..., determined in §8 for the breakdown of the plastic front when propagating without interference from the unloading wave.

To complete the solution, the permanent strain distribution left over the interaction region, using (9·26), is given by

$$\frac{1}{\rho_i c_0^2} k[x_1(t)] = \frac{\sigma_m - \sigma_1(t)}{\rho_i c_0^2} - [\epsilon_m - \epsilon_1(t)]. \tag{9·31}$$

This is the relationship obtained in both types of interaction.

10. Illustration of the interaction-shock formation solution for 24 S-T aluminium

A particular case of the general interaction described in §9 is solved; namely, the overtaking of a plastic loading front by an elastic unloading wave while the continuous plastic wave is breaking down into a shock. A stress-wave profile, which has a parabolic plastic

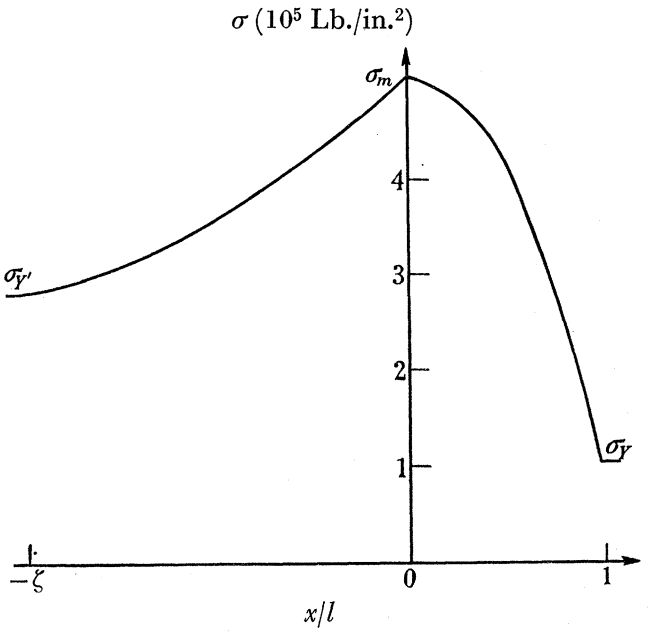

Figure 16. Initial plastic loading-elastic unloading stress-wave profile.

loading front and an exponential elastic unloading front at the start of the interaction, is chosen; the preceding and following waves are replaced by uniform regions since they play no part. The initial stress distribution is given by

$$x \geqslant l: \quad \sigma = \sigma_Y; \tag{10·1}$$

$$\left.\begin{aligned} 0 \leqslant x \leqslant l: &\quad \sigma = F(x) = \sigma_m - (\sigma_m - \sigma_Y)\, x^2/l^2, \\ \sigma_Y \leqslant \sigma \leqslant \sigma_m: &\quad x = \mathscr{F}(\sigma) = l(\sigma_m - \sigma_Y)^{-\frac{1}{2}}(\sigma_m - \sigma)^{\frac{1}{2}}; \end{aligned}\right\} \tag{10·2}$$

$$\left.\begin{aligned} -\zeta l \leqslant x \leqslant 0: &\quad \sigma = G(x) = \sigma_m - \frac{e}{e-1}(\sigma_m - \sigma_{Y'})(1 - \exp[x/\zeta l]), \\ \sigma_{Y'} \leqslant \sigma \leqslant \sigma_m: &\quad x = \mathscr{G}(\sigma) = \zeta l \ln\left[1 - \frac{e-1}{e}\frac{\sigma_m - \sigma}{\sigma_m - \sigma_{Y'}}\right]; \end{aligned}\right\} \tag{10·3}$$

$$x \leqslant -\zeta l: \quad \sigma = \sigma_{Y'}. \tag{10·4}$$

The parameter ζ defines the ratio of the two pulse lengths, and provides a means of varying the time to shock formation in comparison with the interaction duration time. A value is chosen such that the continuous plastic loading front first starts to break down into a shock at some stage during the overtaking by the elastic unloading wave.

It will be shown that breakdown first occurs at the lowest stress point on the plastic front, σ_Y; and the subsequent path of the shock front, $x_s(t)$, as it gradually builds up to cover the whole plastic front, assuming there is no interference from the elastic unloading wave, is obtained by the results (8·37) and (8·38). By choosing a suitable ζ, the elastic unloading wave at first overtakes a section of continuous plastic loading wave front, when the interaction

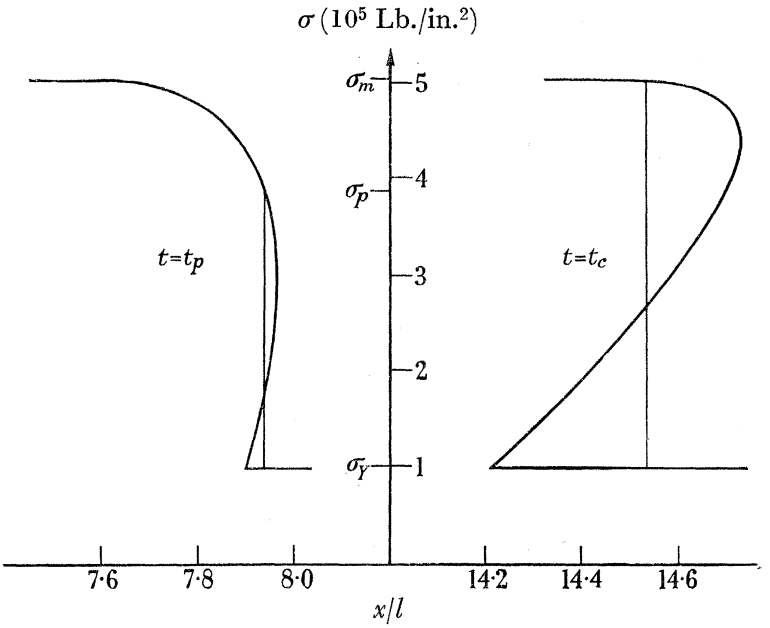

FIGURE 17. Continuous plastic loading stress-wave profile with fitted shock front, at times t_p and t_c.

solution is given by § 6, and then at some stage, $t = t_p$, the interaction line, $x_1(t)$, reaches the shock-front path, $x_s(t)$, after which the interaction proceeds as described in § 9. (The characteristics pattern is shown in figure 5.) In figure 17 is shown the continuous plastic stress-wave profile with fitted shock front at two stages in the breakdown, assuming no interference from the elastic unloading wave. The first is at $t = t_p$, and therefore shows the section of continuous plastic front, to the rear of the shock, which is unloaded during the interaction before the elastic wave interacts with the shock; the second is at $t = t_c$, when the whole plastic front is replaced by a shock. The reflected elastic loading wave-stress profile at the completion of the interaction, $t = t_f$, is shown in figure 18; and the permanent strain distribution over the interaction region is shown in figure 19.

The following values are taken for 24 S-T aluminium; the suffix i denotes the initial conditions before straining:

$$\left.\begin{aligned} &\rho_i = 0{\cdot}1\ \text{Lb./in.}^3, \quad v_i = 0{\cdot}33, \quad \beta = 10{\cdot}632, \\ &\alpha = 29{\cdot}87 \times 10^5\ \text{Lb./in.}^2, \quad \sigma_Y = 1 \times 10^5\ \text{Lb./in.}^2 \end{aligned}\right\} \tag{10·5}$$

The value of g used is 386·4 in./s^2. Now, by (2·31) and (2·52),

$$K_i = \tfrac{1}{3}\alpha\beta = 105{\cdot}9 \times 10^5 \text{ Lb./in.}^2, \tag{10·6}$$

and so

$$E_i = 3K_i(1-2\nu_i) = 108{\cdot}0 \times 10^5 \text{ Lb./in.}^2, \tag{10·7}$$

$$\mu = \text{constant} = E_i/2(1+\nu_i) = 40{\cdot}6 \times 10^5 \text{ Lb./in.}^2 \tag{10·8}$$

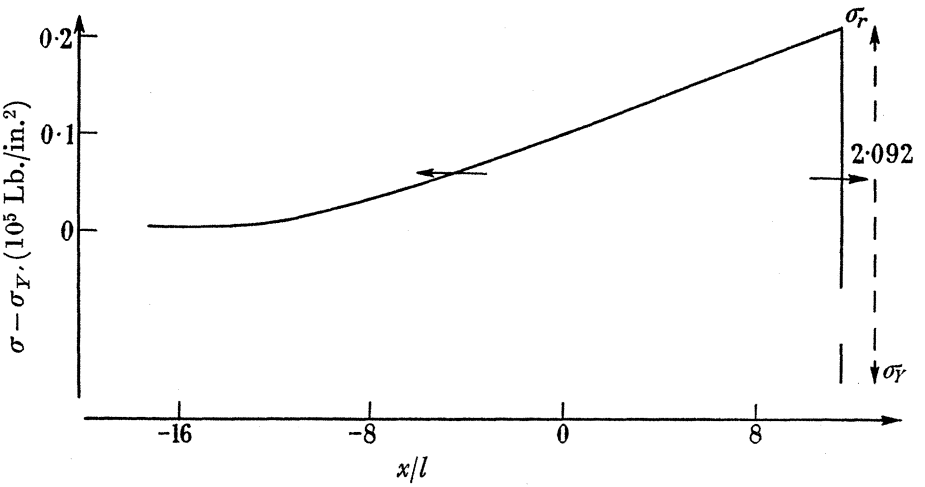

FIGURE 18. Reflected elastic loading stress-wave profile at end of interaction.

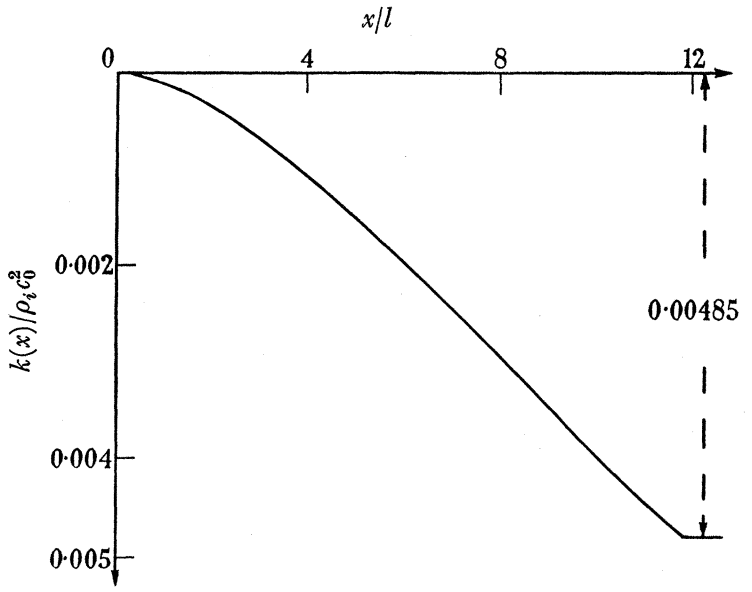

FIGURE 19. The permanent strain distribution over the interaction region.

Comparing (2·29) and (2·31), the elastic stress-strain relationship is given by

$$\frac{\mathrm{d}\sigma}{\mathrm{d}\epsilon} = \frac{\mathrm{d}p}{\mathrm{d}\epsilon} + \frac{4}{3}\frac{\mu}{1-\epsilon}, \tag{10·9}$$

or on integration

$$[\sigma] = [p - \tfrac{4}{3}\mu \ln(1-\epsilon)]; \tag{10·10}$$

and, using (2·33), the plastic loading relation is

$$\sigma - \sigma_Y = p(\epsilon) - p(\epsilon_Y), \tag{10·11}$$

where

$$p = \alpha(1-\epsilon)^{-\frac{2}{3}}\{\exp[\beta\{1-(1-\epsilon)^{\frac{1}{3}}\}] - 1\}. \tag{10·12}$$

Applying (10·10) to the initial elastic loading gives the strain at the elastic limit,

$$\sigma = \sigma_Y = 1 \times 10^5 \text{ Lb./in.}^2,$$

to be

$$\epsilon_Y = 0{\cdot}00617. \tag{10·13}$$

Using (2·40), the yield stress in simple compression is

$$Y = 0{\cdot}495 \times 10^5 \text{ Lb./in.}^2 \tag{10·14}$$

From (2·41), taking a maximum strain

$$\epsilon_m = 0{\cdot}04, \tag{10·15}$$

the strain at the reverse yield point is

$$\epsilon_{Y'} = 0{\cdot}02807. \tag{10·16}$$

Substituting in (10·10), the reverse yield stress is

$$\sigma_{Y'} = 2{\cdot}890 \times 10^5 \text{ Lb./in.}^2, \tag{10·17}$$

and from (10·11), the maximum stress is

$$\sigma_m = 5{\cdot}080 \times 10^5 \text{ Lb./in.}^2 \tag{10·18}$$

The initial stress profiles can now be expressed as

$$\mathscr{F}(\sigma) = 0{\cdot}495l\{10^{-5}(\sigma_m - \sigma)\}^{\frac{1}{2}}, \tag{10·19}$$

$$\mathscr{G}(\sigma) = \zeta l \ln\{1 - 0{\cdot}2886 \times 10^{-5}(\sigma_m - \sigma)\}. \tag{10·20}$$

The elastic wave velocity over the range $\langle \sigma_{Y'}, \sigma_m \rangle$ is taken as

$$c_0 = \left\{\frac{(\sigma_m - \sigma_{Y'})\, g}{\rho_i(\epsilon_m - \epsilon_{Y'})}\right\}^{\frac{1}{2}} = 2{\cdot}663 \times 10^5 \text{ in./s}. \tag{10·21}$$

The value over the initial elastic loading range is

$$c_{0i} = \left\{\frac{\sigma_Y g}{\rho_i \epsilon_Y}\right\}^{\frac{1}{2}} = 2{\cdot}502 \times 10^5 \text{ in./s}. \tag{10·22}$$

By (8·14), the plastic wave velocity is

$$c_1(\epsilon) = \left\{\frac{\alpha\beta g}{3\rho_i}\right\}^{\frac{1}{2}} \{1 + \tfrac{1}{2}d_1\epsilon + (\tfrac{1}{2}d_2 - \tfrac{1}{8}d_1^2)\,\epsilon^2 + \ldots\}, \tag{10·23}$$

thus

$$c_1'(\epsilon) = \left\{\frac{\alpha\beta g}{3\rho_i}\right\}^{\frac{1}{2}} \{\tfrac{1}{2}d_1 + (d_2 - \tfrac{1}{4}d_1^2)\,\epsilon + \ldots\}, \tag{10·24}$$

and so

$$c_1'(\sigma) = \frac{c_1'(\epsilon)}{\mathrm{d}\sigma/\mathrm{d}\epsilon} = \frac{\left\{\frac{\alpha\beta g}{3\rho_i}\right\}^{\frac{1}{2}} \{\tfrac{1}{2}d_1 + (d_2 - \tfrac{1}{4}d_1^2)\,\epsilon + \ldots\}}{\tfrac{1}{3}(\alpha\beta)\,\{1 + d_1\epsilon + \ldots\}}, \tag{10·25}$$

from which

$$\left.\begin{aligned} \frac{1}{c_1'(\sigma)} &\sim \left\{\frac{\alpha\beta\rho_i}{3g}\right\}^{\frac{1}{2}} \frac{2}{d_1}\left\{1 + \left(\tfrac{3}{2}d_1 - 2\frac{d_2}{d_1}\right)\epsilon\right\} \text{ Lb. s/in.}^3, \\ &= 19{\cdot}0\{1 + 2{\cdot}4\epsilon\} \text{ Lb. s/in.}^3. \end{aligned}\right\} \tag{10·26}$$

Therefore $1/c_1'(\sigma)$ is a minimum at the lowest strain point, ϵ_Y. Also

$$-\mathscr{F}'(\sigma) = l/\{2(\sigma_m - \sigma)^{\frac{1}{2}}\,(\sigma_m - \sigma_Y)^{\frac{1}{2}}\} \tag{10·27}$$

is a minimum at the lower limit σ_Y. The time to initial breakdown is therefore, by (8·31)

$$\frac{t_s}{l} = \frac{-\mathscr{F}'(\sigma_Y)}{lc_1'(\sigma_Y)} = 2{\cdot}364 \times 10^{-5}\,\text{s/in.} \tag{10·28}$$

and the shock formation starts at the lowest stress point, σ_Y. The subsequent shock-front path, $x_s(t)$, is determined by the result from §8, which may be expressed as

$$\left.\begin{aligned} t\left\{[\epsilon_1-\epsilon_Y]\,c_1(\epsilon) - \int_{\epsilon_Y}^{\epsilon_1} c_1(\epsilon)\,\mathrm{d}\epsilon\right\} \\ = \int_{\epsilon_Y}^{\epsilon_1} \mathscr{F}(\sigma)\,\mathrm{d}\epsilon - [\epsilon_1-\epsilon_Y]\,\mathscr{F}(\sigma_1), \\ x_s(t) = \mathscr{F}(\sigma_1) + tc_1(\sigma_1), \end{aligned}\right\} \tag{10·29}$$

where (σ_1, ϵ_1) is the state immediately behind the shock front at time t. The position of the shock at the start of breakdown is

$$x_s(t_s)/l = 5{\cdot}865. \tag{10·30}$$

If there were no interaction, the whole plastic front would be replaced by a shock at a time t_c such that

$$t_c/l = t(\sigma_m)/l = 6{\cdot}425 \times 10^{-5}\,\text{s/in.}, \tag{10·31}$$

$$x_s(t_c)/l = 14{\cdot}540. \tag{10·32}$$

The elastic unloading wave overtakes at first a section of continuous plastic wave front, until at some stress level, σ_p, the interaction line, $x_1(t_p)$, reaches the shock front, $x_s(t_p)$; the interaction path is subsequently the shock-front path. For a sequence of strain values, ϵ_1, on the plastic front, the corresponding values of σ_1, $c_1(\epsilon_1)$, $\sigma_u(\sigma_1)$, are calculated. The interaction is completed when $\sigma_u(\sigma_1)$ decreases to $\sigma_{Y'}$, that is, at $\sigma_1 = \sigma_r$ which is found to be

$$\sigma_r = 3{\cdot}092 \times 10^5\,\text{Lb./in.}^2 \tag{10·33}$$

The corresponding strain is

$$\epsilon_r = 0{\cdot}02432. \tag{10·34}$$

Thus

$$\frac{\sigma_m-\sigma_r}{\sigma_m-\sigma_{Y'}} = \frac{1{\cdot}988}{2{\cdot}190} = 0{\cdot}908, \tag{10·35}$$

and so the plastic front is reduced by roughly 90 % of the unloading wave amplitude. Expressing the ratio as $2\bar{c}_1/(c_0+\bar{c}_1)$ gives

$$\bar{c}_1 = 2{\cdot}214 \times 10^5\,\text{in./s}, \tag{10·36}$$

which agrees closely with the average value of the plastic wave velocity over the range (σ_r, σ_m). It would be sufficient to take the plastic wave velocity as this fixed value to obtain quite accurate values of the wave amplitudes, but the approximation would effect slightly the function $x_1(t)$, and consequently the wave profiles; furthermore, shock formation could not be treated by this method.

The value $\zeta = 2$ is taken, and this gives the position of the interaction line as it reaches the shock front to be

$$x_1(t_p)/l = 7{\cdot}953. \tag{10·37}$$

The corresponding values of t_p, σ_p and ϵ_p are

$$\left.\begin{aligned} t_p/l &= 3{\cdot}357\times10^{-5}\,\text{s/in.},\\ \sigma_p &= 3{\cdot}828\times10^{5}\,\text{Lb./in.}^2,\\ \epsilon_p &= 0{\cdot}03030. \end{aligned}\right\} \tag{10·38}$$

The velocity of the shock front relative to the material ahead, using (9·17), is then

$$-q_0(\sigma_p) = 2{\cdot}115\times10^{5}\,\text{in./s}, \tag{10·39}$$

and is assumed to remain constant throughout the subsequent interaction; this was shown in § 9 to be a good approximation. The end of the interaction is then given by

$$\left.\begin{aligned} t_f/l &= 5{\cdot}207\times10^{-5}\,\text{s/in.},\\ x_1(t_f)/l &= 11{\cdot}866. \end{aligned}\right\} \tag{10·40}$$

An extract from the various quantities calculated, showing the more relevant functions, is given in table 1. The function $-k(x_1)/\rho_i c_0^2$ represents the permanent strain distribution left

TABLE 1

ϵ_1	σ_1 (10^5 Lb./in.^{2})	$c_1(\epsilon_1)$ (10^5 in./s)	$\sigma_u(\sigma_1)$ (10^5 Lb./in.^{2})	$\frac{x_s(\sigma_1)}{l}$	$\frac{x_1(\sigma_1)}{l}$	$\frac{-k(x_1)}{\rho_i c_0^2}$
0·0400(ϵ_m)	5·080	2·263	5·080	14·540	0·000	0·000000
0·0390	4·946	2·256	4·935	11·596	1·661	0·000270
0·0380	4·815	2·249	4·792	10·733	2·585	0·000556
0·0370	4·685	2·243	4·650	10·115	3·393	0·000848
0·0350	4·428	2·230	4·367	9·335	4·823	0·001448
0·0330	4·169	2·218	4·085	8·650	6·203	0·002037
0·0310	3·916	2·206	3·855	8·105	7·322	0·002659
0·03030(ϵ_p)	3·828	—	—	7·953	7·953	—
0·0290	3·665	2·193	3·528	7·769	8·732	0·003292
0·0270	3·418	2·181	3·259	7·449	9·906	0·003046
0·0250	3·174	2·168	2·982	7·231	11·327	0·004617
0·02432(ϵ_r)	3·092	2·164	2·890	—	11·866	0·004850
0·0230	2·932	2·157	—	6·884	—	—
0·0210	2·692	2·144	—	6·704	—	—
0·0190	2·453	2·133	—	6·416	—	—
0·0170	2·219	2·121	—	6·394	—	—
0·0150	1·988	2·109	—	—	—	—
0·0130	1·760	2·097	—	6·293	—	—
0·0110	1·535	2·085	—	—	—	—
0·0090	1·312	2·074	—	5·920	—	—
0·00617(ϵ_Y)	1·000	2·058	—	5·865	—	—

over the interaction region $0\leqslant x/l\leqslant 11{\cdot}866$. In this case, the plastic strain component decreases by an amount 0·00485 over the region. The strain decrease over the elastic unloading wave is $\epsilon_m-\epsilon_{Y'}=0{\cdot}01193$, and the strain reduction on the plastic front is $\epsilon_m-\epsilon_r=0{\cdot}01568$.

The author wishes to express his gratitude to Professor M. J. Lighthill and Mr D. R. Bland for their guidance and criticism during the course of the work.

References

Bridgman, P. W. 1949*a* *Proc. Amer. Acad. Arts Sci.* **77**, 187.
Bridgman, P. W. 1949*b* *The physics of high pressure*, p. 386. London: Bell and Sons.
Broberg, K. B. 1955 *J. Appl. Mech.* **22**, 317.
Donnell, L. H. 1930 *Trans. Amer. Soc. Mech. Engrs*, **52**, 153.
Hawkyard, J. B. & Freeman, P. 1951 *B.I.S.R.A. Rep.* MM/E/51/51.
Hill, R. 1950 *The mathematical theory of plasticity*. (Introduction.) Oxford: Clarendon Press.
Johnson, J. E., Wood, D. S. & Clark, D. S. 1953 *J. Appl. Mech.* **20**, 513.
Karman, T. von, Bohnenblust, H. F. & Hyers, D. H. 1942 N.D.R.C.A-103, O.S.R.D. 946.
Koehler, J. S. & Seitz, F. 1944 O.S.R.D. 3230.
Lee, E. H. 1952 *Quart. Appl. Math.* **10**, 335.
Lee, E. H. & Tupper, S. J. 1954 *J. Appl. Mech.* **21**, 335.
Lighthill, M. J. 1956 *Surveys in mechanics*, p. 306. Cambridge University Press.
Mallory, D. H. 1955 *J. Appl. Phys.* **26**, 555.
Pack, D. C., Evans, W. M. & James, H. J. 1948 *Proc. Phys. Soc.* **60**, 1.
Taylor, G. I. & Farren, W. S. 1925 *Proc. Roy. Soc.* A, **107**, 422.
Walsh, J. M. & Christian, R. H. 1955 *Phys. Rev.* **97**, 1544.
White, M. P. & Griffis, L. Van. 1947 *J. Appl. Mech.* **14**, A 337.
White, M. P. & Griffis, L. Van. 1948 *J. Appl. Mech.* **15**, 256.
White, M. P. & Griffis, L. Van. 1949 *J. Appl. Mech.* **16**, 39.
Wood, D. S, 1952 *J. Appl. Mech.* **19**, 521.

PHILOSOPHICAL TRANSACTIONS OF THE ROYAL SOCIETY A MATHEMATICAL, PHYSICAL & ENGINEERING SCIENCES